universität wien

# DIPLOMARBEIT

## Identification of factors involved in mammalian X chromosome inactivation

angestrebter akademischer Grad

Magistra der Naturwissenschaften (Mag. rer.nat.)


| | |
|---|---|
| Verfasserin: | Renate Härtel |
| Matrikel-Nummer: | 9949191 |
| Studienrichtung: | Molekulare Biologie (A490) |
| Betreuer: | Anton Wutz |


Wien, November 2008-11-25

# Zusammenfassung

X-Chromosom-Inaktivierung ist der Vorgang, bei dem die unterschiedlichen Genmengen zwischen weiblichen (XX) und männlichen (XY) Säugern kompensiert wird. Bei weiblichen Säugetieren wird während der frühen Entwicklung ein X Chromosom transkriptionell abgeschalten und bildet den sogenannten ´Barr body´. Dieser Inaktivierungsvorgang wird von der *Xist* RNA initiiert, welche sich über das gesamte Chromosom ausbreitet von dem sie transkribiert wird. Während der frühen embryonalen Entwicklung ist *Xist* notwendig für die Initiierungsphase des Inaktivierungsvorganges. Später in der Differenzierung, in der sogenannten ´Aufrechterhaltungsphase´, wird der inaktive Status des Chromosoms irreversibel und unabhängig von der Expression von *Xist.* Obwohl bereits einige Faktoren, die durch die Expression von *Xist* rekrutiert werden, identifiziert wurden, ist der Mechanismus, der den Übergang von der Initiierungs- zur Aufrechterhaltungsphase einleitet, noch nicht geklärt.

In der Initiierungsphase werden Histone modifiziert, während in der Aufrechterhaltungsphase Proteine, wie Saf-A, Ash2 und macroH2A rekrutiert werden und Histon H4 hypacetyliert wird. Die Rekrutierung von Saf-A, Ash2 und macroH2A und die Modifizierung von Histonen sind abhängig von der Expression von *Xist,* benötigen jedoch des weiteren das sogenannte ´Chomosomale Gedächtnis´, welches eine spezifische chromosomale Veränderung am X Chromosom darstellt.

Diese Veränderung, welche während der frühen ES Differenzierung am X-Chromosom etabliert wird, ist bis jetzt auf molekularer Ebene ungeklärt. Deacetylierung von Histon H4 besitzt Eigenschaften, die mit jenen des ´Chromosomalen Gedächtnisses´ korrelieren und könnte daher eine Komponente des ´Gedächtnisses´ darstellen.

Im ersten Teil dieser Arbeit wurde die Deacetylierung von Histon H4 als potentielle Kandidatin für die molekulare Veränderung des `Chromosomalen Gedächtnisses´ untersucht. Hierbei wurden die Effekte auf das ´chromosomale Gedächtnis´ nach chemischer Inhibierung der Histon Deacetylasen untersucht. Die Resultate dieser Studie deuten darauf hin, dass die Klasse III der Histon Deacetylasen potentiell mit der Bildung des ´Chromosomalen Gedächtnisses´ involviert ist.

Im zweiten Teil dieser Arbeit wurde ein biochemischer Ansatz für die Identifizierung von Faktoren, welche in der Initiierungsphase durch *Xist* rekrutieren, erforscht.

Das Ausbreiten der *Xist* RNA über das gesamte X Chromosom in der Initiierungsphase vermittelt eine transkriptionelle Inaktivierung des Chromatins, ist aber alleine nicht ausreichend für die Repression der Gene. Die Faktoren, welche mit *Xist* kooperieren um das anfängliche Stilllegen der Gene zu bewerkstelligen, sind bis dato nicht bekannt.

In unserer Studie haben wir ein Verfahren für eine biochemische Fraktionierung der nuklearen Matrix, welche bekanntermaßen die *Xist* RNA beinhaltet, entwickelt. Die Untersuchung dieser Fraktion machte es möglich Proteine zu detektieren, die sich durch X-Inaktivierung anreichern.

Eine massenspektrometrische Analyse dieser Proteinproben identifizierte die Anreicherung von Trim28 in ES-Zellen durch die Expression von *Xist*. Trim28 spielt eine Rolle beim Stilllegen retroviraler Gene in ES-Zellen (Wolf und Goff, 2007). Daher, deuten die vorläufigen Ergebnisse dieser Arbeit darauf hin, dass Trim28 einen interessanten Kandidaten für den Mechanismus der X-Inaktivierung darstellt. Weitere Studien, wie genetische Ansätze, werden notwendig sein, um das Involvieren von Trim28 in der X-Chromosom-Inaktivierung zu testen.

# Summary

X chromosome inactivation is the process that compensates the different gene dosages between females (XX) and males (XY) in mammals. During early mammalian development one X chromosome becomes transcriptionally silent, which leads to the formation of the so called Barr body. This silencing process is triggered by *Xist* RNA, which initially spreads over one chromosome from which it is transcribed. *Xist* is required for initiation of X inactivation early in development during the so called initiation phase. Later in differentiation silencing becomes irreversible and independent of *Xist* during the maintenance phase. Albeit, several factors have been identified that are recruited by *Xist* in the maintenance phase, the mechanism for the transition from initiation to maintenance of X inactivation is presently unknown. During the process of X inactivation, histones are modified in the initiation phase and the recruitment of Saf-A, Ash2, macroH2A and hypoacetylated histone H4 mark the maintenance phase. The recruitment of Saf-A, Ash2, macroH2A and histone modifications are dependent on *Xist* expression and in differentiation a molecular change on the X chromosome is triggered that has been termed ´chromosomal memory´. The molecular basis of this chromosomal change, which is established early in ES differentiation, is presently unknown. Deacetylation of histone H4 represents a chromatin feature that correlated with memory and could be a component of its mechanism.

In the first part of this work deacetylation of histone H4 was investigated as chromatin feature that correlates with memory. Its role as a component of the memory mechanism was tested using chemical inhibition of histone

deacetylation. The results of this study suggest that class III histone deacetylases could potentially be involved in the formation of memory.

In the second part of this work a biochemical approach was explored for the identification of factors that are recruited by *Xist* for the initiation of X inactivation. During the process of X inactivation, initial spreading of *Xist* RNA mediates the formation of silent chromatin, but is not sufficient for gene repression. The factors that cooperate with *Xist* the initial establishment of silent chromatin are presently unknown. In our study, we established a biochemical fractionation procedure of the nuclear matrix fraction, which is known to contain *Xist* RNA, to detect proteins that become enriched in the matrix fraction upon X inactivation. Mass spectrometric analysis of protein samples identified an enrichment of Trim28 in ES cells upon *Xist* expression. Trim28 has been implicated in retroviral silencing in ES cells (Wolf and Goff, 2007). Thus, the preliminary findings of this work suggest Trim28 as an interesting candidate for the mechanism of X chromosome silencing. Future work including genetic studies will be required to test a potential involvement of Trim28 in X inactivation.

# Table of Contents

## Dosage compensation systems

Different sex determination systems have evolved throughout the animal kingdom. Environmental sex determination (such as systems based on ambient temperature) and genetic sex determination are used by closely related species. Sex determination by sex chromosomes can be observed in worms, insects and vertebrates. One of the sex chromosomes has become structurally modified and limited to one sex. The other sex chromosome has remained structurally unchanged. Depending on the species, the structurally modified chromosome is transmitted from males to sons (Y chromosome) or from females to daughters (W chromosome). Therefore either males (XY) or females (ZW) can be heterogametic. The unmodified chromosome is present in two doses in the homogametic sex, which results in an inequality in the dosage of the genes, present on the X or Z chromosomes in males and females. Many of these genes are equally important for the development and maintenance of both males and females. Therefore different gene dosages of both sexes would lead to a variation in gene expression levels, which might result in differential selection between the sexes. To compensate for differences in the dosage of X-linked or W-linked genes between the sexes, mechanisms have evolved to prevent such inequalities.

The mechanisms that are employed to achieve dosage compensation of gene expression of X or W linked gene products are remarkably different throughout the animal kingdom. The phenomenon of dosage compensation was

discovered in Drosophila by Herman Muller more than 70 years ago. To date, dosage compensation mechanisms have been extensively studied in three very distantly related species: mammals, Caenorhabditis *elegans* and Drosophila *melanogaster*. These organisms achieve the transcriptional regulation leading to equal gene expression in different ways. In Drosophila the level of transcription of the single male X chromosome is increased 2-fold to equalize gene expression of XX females (Akhtar, 2003). C. *elegans* decreases the level of transcription of the two doses of X-linked genes in hermaphrodites to achieve dosage compensation to X0 males (Meyer, 2000). In mammals the two X chromosomes are treated differently in female cells: The inactivation of one of the two female X chromosomes compensates the dosage of X-linked genes between the sexes.

The study of dosage compensation provides a unique window into a variety of fundamental mechanisms of transcriptional regulation.

# X chromosome inactivation compensates X chromosome gene dosage in mammals

## X chromosome inactivation

Several observations provided the basis for Mary F. Lyon´s pioneering theory of X chromosome inactivation in mammals (Lyon, 1961): The observation of a dense staining nuclear structure in neuronal nuclei of female cats in 1949 was the first evidence for mammalian X chromosome inactivation (Barr and Bertram, 1949). Later it was discovered that this ´sex chromatin body´ or Barr body, which was observed in nuclei of somatic cells of females, corresponds to an X chromosome (Ohno and Hauschka, 1960). This observation laid the cornerstone of the study of dosage compensation in mammals, which demonstrated that one of the two X chromosomes in female cells is randomly inactivated through transcriptional silencing thereby equalizing the expression of X-linked genes between XX females and XY males (Lyon, 1961). Further, it was demonstrated that female mice showed a spotted phenotype due to a translocation of an autosomal coat colour gene to the X chromosome (Russell, 1963). Detailed analysis of X; A translocations resulted in the identification of a *cis*-acting DNA element regulating X chromosome inactivation. This element was named the X chromosome inactivation centre (*Xic*). The *Xic* was defined as a 700 kb – 1200 kb region using translocations involving the X chromosome that were able to induce silencing of autosomal coat colour genes. When translocated to an

autosome the *Xic* triggered an ectopic inactivation event (Rastan, 1983; Rastan and Robertson, 1985). A more recent study identified the localization of the *Xic* to (Brown et al., 1989). This facilitated the discovery of a gene encoding a nontranslated RNA, X inactive-specific transcript or *XIST* that is transcribed only by the inactive chromosome (Brown et al., 1991a; Brown et al., 1991b; Brown, 1991). The observation that *XIST* is a noncoding RNA, which localizes to the chromatin of inactive X (Brown et al., 1992), suggested that it might be involved in the silencing process. The *Xic* contains the genetic information for counting, choice and the silencing process itself. Counting is a process whereby the X;A ratio is measured and only one single X chromosome per diploid autosome set remains active. The *Xic* elements required for counting were mapped to *cis* acting sequence lying 5´ and 3´ to *Xist* (Augui et al., 2007; Herzing et al., 1997). Deletion of 65 kb in the region 3´ to the *Xist* gene leads to inappropriate X chromosome inactivation even in male cells with a single X (Morey et al., 2004). This demonstrates that counting is achieved only by the *Xic* region. The choice of the X chromosome that will undergo X inactivation is influenced by multiple elements spreading across the *Xic* region. The *Xic* contains 12 transcription units, seven of which are not involved in X inactivation (Xptc, Cnbp2, Tsx, Chic1, Cdx4, Nap1/2 and Ppnx). The *Xic* is very characteristic in its high abundance of genes encoding non-coding RNAs (Xist, Tsix, Ftx, Jpx) (Rougeulle and Avner, 2003).

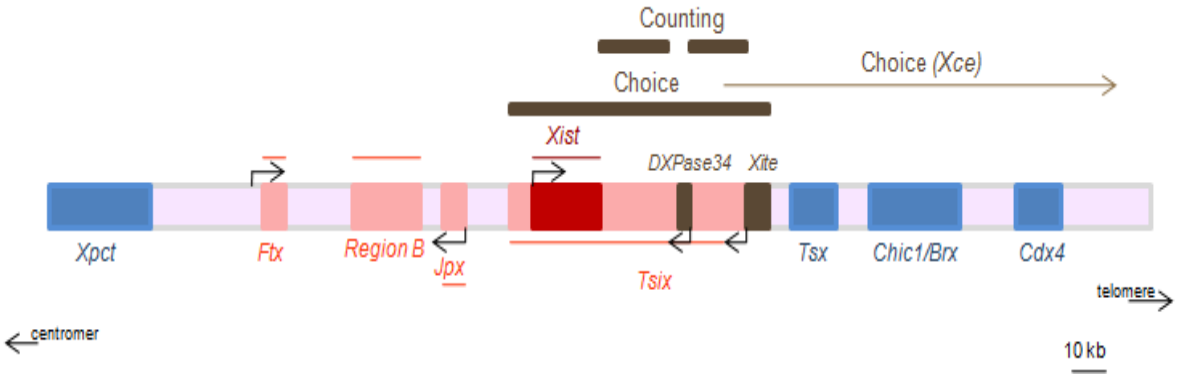


**Figure 1: Transcriptional map of the X inactivation centre (*Xic*)**

Genes shown in red produce non-coding transcripts and genes shown in blue produce protein-coding transcripts and have no known *Xic* related function. Regions shown in brown show elements involved in counting and choice.

## The *Xist* gene is required for X chromosome inactivation

The fist gene, which was mapped to the *Xic* was the *Xist* gene. It encodes a 17 kb long non-coding spliced RNA that is exclusively expressed from the inactive X chromosome (Borsani et al., 1991; Brockdorff et al., 1991; Brown et al., 1991a; Brown et al., 1991b).

Deletions at the *Xist* locus showed that this gene is absolutely required for the initiation of X inactivation in *cis* (Marahrens et al., 1997; Penny et al., 1996). *Xist* is expressed at low levels in undifferentiated female ES cells. In cells that contain more than one *Xic*, *Xist* expression is upregulated on the future inactive X chromosome after one to two days of ES differentiation. *Xist* RNA physically interacts with the chromatin in *cis* and covers the entire chromosome from which it is transcribed, suggesting that it could serve as a recruitment factor for

additional molecules that are essential for X chromosome inactivation (Clemson et al., 1996; Wutz, 2003). Transcriptional silencing occurs between one or two cell cycles after RNA coating (Wutz and Jaenisch, 2000). This indicates that *Xist* is directly responsible for mediating gene silencing. *Xist* expression at later stages of differentiation no longer causes silencing anymore. Thus, its function is developmentally restricted (Wutz and Jaenisch, 2000). Chromosomal coating of *Xist* RNA does not depend on specifically on features of the X chromosome as *Xist* also interacts with chromatin in *cis* when expressed from an autosome (Wutz and Jaenisch, 2000). Recent studies showed that *Xist* co-localizes with the nuclear matrix protein scaffold attachment factor A (Saf-A) (Fackelmayer, 2005; Helbig and Fackelmayer, 2003), indicating that the nuclear matrix could contribute to *Xist* localization to the X chromosome. *Xist* localization is cell cycle dependent (Clemson et al., 1996). In mouse cells, *Xist* detaches from the Xi at the transition from metaphase to anaphase and is coating the same chromosome when the cells re-enters G1 phase.

Further observations showed that the localization along the length of the X chromosome and the silencing ability of *Xist* RNA are functionally separable (Wutz et al., 2002).

Identification of factors that bind to the different functional regions of the *Xist* RNA will provide more insight into the mechanism of silencing.

## The repeat- A motif at the 5´end is essential for gene silencing

First cloning and sequencing studies of the mouse *Xist* gene revealed that the full-length 15 kb transcript contains no significant conserved open reading frame (ORF) (Brockdorff et al., 1992). Further sequencing analysis of the *Xist* gene revealed significant conservation over five short regions and *Xist* specific tandem repeats. However, the *Xist* genes of different mammals show low overall sequence conservation (Nesterova et al., 2001). Experimental evidence of the functionality of direct repeat sequences were observed by deletion analysis of mouse *Xist* RNA (Wutz et al., 2002). Deletion of the highly conserved sequence motif at the 5´end, the so called ´A-repeat´, resulted in a mutant RNA that is unable to induce gene silencing without affecting *Xist* localization to chromatin (Wutz et al., 2002). Further it was shown that macroH2A1 localizes to the X chromosome independently of silencing. This indicates that the ´A-repeat´ is essential for the initiation of XCI, but is not required for recruitment of factors to the inactive X chromosome. In contrast to the defined domain, that is required for silencing, regions for *Xist* localization are scattered throughout *Xist* and are functional redundant (Wutz et al., 2002).

## A shift from reversible to irreversible gene silencing

The development of an inducible *Xist* expression system in male ES cells made it possible to experimentally control the initiation of chromosome-wide silencing in ES cell differentiation. In this system the transactivator for the TetON system is fused to a nuclear localization signal (nlsrtTA) and further knocked into the Rosa26 locus on chromosome 6 by homologous recombination (Gossen et al., 1995; Wutz and Jaenisch, 2000). Addition of doxycycline induces the expression of *Xist* cDNA transgene (Wutz and Jaenisch, 2000). In undifferentiated ES cells induction of *Xist* expression causes efficient, but reversible gene silencing. Silencing is restricted to the chromosome containing the *Xist* transgene and requires continuous *Xist* expression. After 48 hours of ES cell differentiation an epigenetic transition occurs on the chromosome that makes chromatin irresponsive to *Xist.* One cell division later, after passing a ´critical window´ of XCI at 72 hrs of differentiation, silencing becomes irreversible and is maintained by redundant mechanisms even in the absence of *Xist* expression.

These experiments indicated that during the initiation phase of X inactivation, *Xist* causes efficient, but reversible gene silencing. *Xist* is no longer required for maintenance of the inactive state. Upon differentiation a transition to a chromatin state occurs that establishes irreversible gene silencing and maintenance of XCI (Wutz and Jaenisch, 2000).

## X inactivation is a multi-step process

X chromosome inactivation is a developmentally regulated process. It can be recapitulated in female ES cells. Studying ES cell differentiation provided insight into the epigenetic events during X chromosome inactivation. XCI starts with the accumulation of *Xist* along the entire future inactive X chromosome and the exclusion of the transcription machinery from the Xi chromosome territory. RNA polymerase II, splicing factors and nascent transcripts are absent from the *Xist* covered chromosome. Subsequently, Polycomb repressor complex 1 (PRC1) and 2 (PRC2) are recruited to the inactive X and mediate histone modifications such as ubiquitinylation of histone H2A lysine 119 and tri-methylation of histone H3 lysine 27 (H3K27me3). During this initiation phase of XCI *Xist* triggers silencing. If cell differentiation progresses histone macro H2A, Saf-A and Ash2 becomes enriched on the Xi. Further, histone H4 becomes hypoacetylated. During this maintenance phase *Xist* is not required for the silent state.

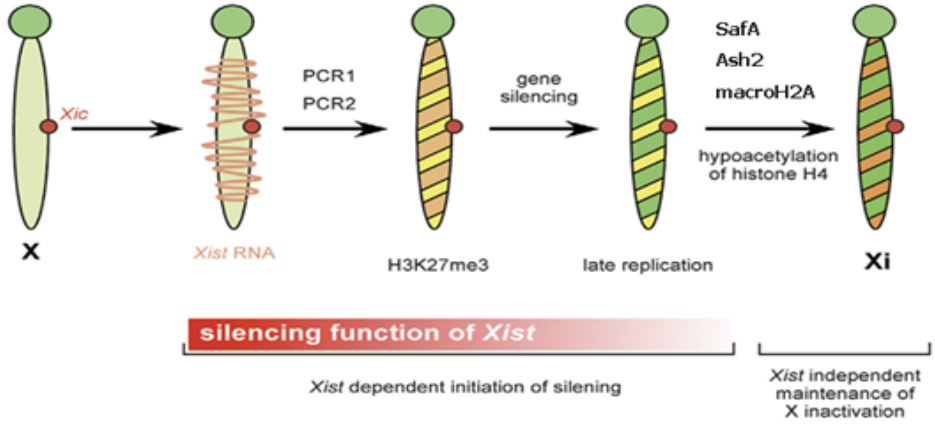


**Figure 2: X chromosome silencing is a multistep process**

Initially, *Xist* RNA spreads over the whole chromosome from which it is transcribed. *Xist* RNA accumulation is followed by recruitment of Polycomb repressor complex 1 and 2 which mediate histone modifications as trimethylation of H3K27. As cell differentiation progresses histone H4 becomes hypoacetylated and the proteins SafA, Ash2, and macroH2A recruit to the inactive X. This silencing process can be divided in 2 phases. The initiation phase, which is reversible and *Xist* dependent followed by the maintenance phase which is irreversible and independent of *Xist* expression.

## A chromosomal memory is triggered by *Xist* in ES differentiation

*Xist* is able to induce chromosome-wide silencing at early timepoints in ES cell differentiation. During differentiation *Xist* loses its potential for initiation of gene silencing. In somatic cells such as embryonic fibroblasts forced expression of *Xist* does not trigger silencing (Wutz and Jaenisch, 2000). During cellular differentiation silencing of the inactive X becomes irreversible and independent of *Xist* (Csankovszki et al., 2001; Marahrens et al., 1998; Penny et al., 1996). Thus, X

inactivation can be separated into an initiation phase, when initiation of silencing depends on *Xist*, and a maintenance phase that is independent of *Xist*.

The mechanism that underlies the transition to the maintenance phase and the factors that are involved in this process are presently unknown. During the process of X inactivation, the recruitment of a variety of different factors and posttranslational modifications are involved. Early in ES cell differentiation *Xist* recruits the Polycomb group complex 2 to the inactive X chromosome mediating tri-methylation of histone H3 lysine 27 (H3K27me3). Recruitment of PcG complexes requires *Xist* RNA. Thus, the PcG associated histone modifications are reversible and are lost when *Xist* expression is disrupted. Turning off *Xist* during maintenance phase resulted in low levels of H3K27me3 (Kohlmaier et al., 2004). *Xist* is not sufficient for PcG recruitment in differentiated cells. The maintenance of efficient H3K27me3 late in ES cell differentiation is dependent on a ´chromosomal memory´. Studying H3K27me3 in male ES cells carrying an inducible *Xist* cDNA transgene showed that *Xist* expression in an early time window in ES cell differentiation is essential for efficient PcG recruitment later in differentiation. H3K27me3 was detected when *Xist* was induced before 3 days of differentiation. However, induction of *Xist* from later timepoints led to inefficient recruitment of PcG complexes and histone modifications.

These studies also revealed that continuous expression of *Xist* was not required for efficient recruitment in differentiated cells. When *Xist* was induced early, efficient H3K27me3 could be established in differentiated cells when *Xist* was reexpressed even after a period of no *Xist* expression. Since continuous *Xist* expression and continuous H3K27me3 were not required it was proposed that a memory had been established after 3 days of differentiation that could be

maintained independent of *Xist* (Kohlmaier et al., 2004). This study indicates that a molecular change on the X chromosome, termed the chromosomal memory, which is established upon early *Xist* expression and stays independent of *Xist* during maintenance phase correlates with the transition to the maintenance phase (Kohlmaier et al., 2004).

Previously, it has been shown that the recruitment of the TrxG protein Ash2l, Saf-A and macroH2A occurs concurrently with memory imposition in ES cell differentiation. Similar to tri-methylation of H3K27, *Xist* expression during early differentiation also regulates efficient recruitment of Saf-A, Ash2 and macroH2A (Pullirsch 2008).

## Histone deacetylation as a potential mechanism for chromosomal memory

The recruitment of Saf-A, Ash2, macroH2A and histone modifications such as H3K27me3 and H2AK119ub1 are dependent on *Xist* expression and in differentiated cells require a molecular change on the X chromosome. This chromosomal change is established by *Xist* expression during and early timewindow in ES cell differentiation and is called the ´chromosomal memory´. Presently, the molecular basis of this X chromosomal memory is unknown.

Notably, it was shown that in differentiated cells *Xist* mediated H2A ubiquitination is regulated by a memory but is not dependent on gene silencing (Schoeftner et al., 2006). Further studies demonstrated that Saf-A, Ash2 and

macroH2A are recruited to the X chromosome upon early *Xist* expression in differentiated ES cells that lack the A repeat responsible for silencing (Pullirsch, 2008). These studies indicate that the establishment of memory is independent of gene silencing and that the mechanism of memory is different from the formation of a silent heterochromatic X chromosome.

Conditional deletion of *Xist* RNA in mouse embryonic fibroblasts demonstrated that in the absence of *Xist*, hypoacetylation on histone H4 is maintained on the inactive X chromosome (Csankovszki et al., 1999). Analysis on the timing of histone H4 hypoacetylation showed that a hypoacetylated X chromosome was established by *Xist* in ES cells after 3 days of differentiation (Chaumeil et al., 2002; Keohane et al., 1996). Remarkably, a hypoacetylated X chromosome was detected in ES cells expressing a silencing deficient *Xist* after 3 days of differentiation, which was stably maintained after Xist was turned off on day 4 of differentiation (Pullirsch, 2007). These data demonstrate that hypoacetylation of histone H4 occurs at the time when memory is established and can be maintained independent of *Xist* and gene repression, indicating a correlation of H4 hypoacetylation with memory in X inactivation.

Histone deacetylases (HDACs), which catalyze the removal of acetyl groups from the N-terminal tails of histones, can be divided phylogenetically into three classes based on their homology to *Saccharomyces cerevisiae* HDACs: Rpd3 (class I), Hda1 (class II) and Sir2 (class III). Class I and II both require the presence of a zinc ion for hydrolysis of the acetyl group. Upon deacetylation both release the acetyl group in the form of acetate. In contrast, Sir2 requires the presence of the metabolic cofactor $NAD^+$ for deacetylation. The acetyl group is

removed from the histone by an ADP-ribosyl transferase reaction, which transfers the acetyl group to ADP ribose (Ekwall, 2005).

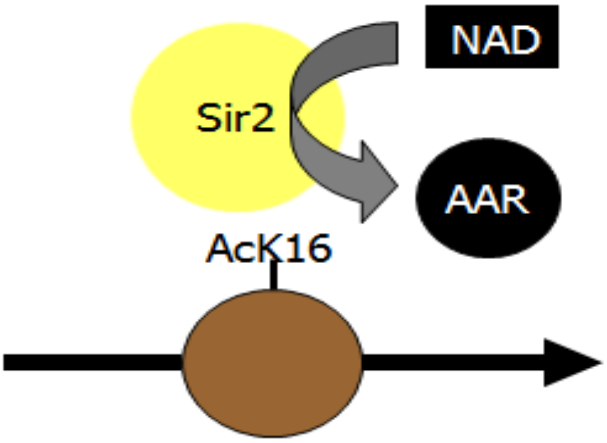


**Figure 3: Sirt2 deacetylation**

In the presence of an acetylated lysine (K) substrate, Sir2 catabolises the NAD molecule into activated ADP-ribose and nicotinamide. The latter product is released. The enzyme catalyses the transfer of the acetyl group to ADP-ribose, resulting in a deacetylated substrate and a novel compound, O-acetyl-ADP ribose (AAR), as final product.

S. cerevisiae Sir2 is involved in the epigenetic silencing of three main loci in budding yeast: mating type loci, telomeres and nucleolar rDNA tandem repeats (Guarente, 1999). Sir2 hypoacetylates lysine 16 on the N-terminal tails of histone 4, which is a mark of Sir2 silencing (Guarente, 1999; Robyr et al., 2002). The product of the deacetylation reaction is O-acetyl-ADP ribose, which is probably required for spreading of the Sir complex on chromatin since it changes the conformation of Sir3 and promotes its binding to Sir2/Sir4 dimers in vitro (Liou et al., 2005). Interestingly, it was observed in mammalian systems, that O-acetyl-ADP ribose can bind to macroH2A which is recruited to the inactive X chromosome in maintenance phase (Kustatscher et al., 2005).

## Factors involved in the initiation phase of X inactivation

Several early alterations in chromatin structure occur during the initiation phase of X inactivation. The expression of *Xist* RNA triggers these epigenetic changes. Asynchronous replication of the two X chromosomes in female cells is observed early after *Xist* has covered the chromosome. This contrasts with the behaviour of homologous autosomes, which replicate at the same time in S-phase (Morishima et al., 1962). Late replication is a classic marker for the silent X chromosome (Csankovszki et al., 2001; Takagi et al., 1982).

Several recent studies have focused on the action of *Xist* early in differentiation and identified the loss of euchromatin-associated histone modifications such as acetylation of histone H3 lysine 9 (H3K9Ac) and di- and tri-methylation of histone H3 lysine 4 (H3K4me2, H3K4me3) (Chaumeil et al., 2002; Heard et al., 2001; Okamoto et al., 2004). However, it is not clear if this early disappearance of histone marks is a passive effect of replication or an active removal by enzymatic or proteolytic factors.

Immediately following these changes, polycomb group proteins appear on the *Xist* coated chromosome mediating histone modifications such as dimethylation of histone H3 lysine 9, monomethylation of histone H4 lysine 20 and ubiquitination of histone H2A (de Napoles et al., 2004; Heard et al., 2001; Kohlmaier et al., 2004; Plath et al., 2003; Silva et al., 2003). Global H4 hypoacetylation occurs shortly afterwards and marks the maintenance phase of X inactivation.

The first discovery of Polycomb group proteins as important silencing factors was made in Drosophila (Simon and Tamkun, 2002). Two large Polycomb repressive complexes (PRCs) were identified in mammals: PRC2 is thought to be involved in the initial maintenance of the repressed states and the PRC1 complex is thought to act subsequently to, and synergistically with PRC2. The role of the histone modifications catalyzed by PRC1 and PRC2 is presently unknown. The histone methyl-transferase PRSet7 was suggested to mediate H4K20me1. G9a was suggested as a likely candidate for H3K9 dimethylation, although no alteration on the inactive X chromosome was observed in *G9a*-knock-out mice embryos (Ohhata et al., 2004). The establishment of H3K27me3 and H4K20me1 was observed in ES cells expressing a silencing-deficient *Xist* RNA. This indicates that histone modifications, which mark the silent chromatin, are not sufficient to initiate gene silencing during X chromosome inactivation. Possibly, the initiation and maintenance of gene silencing requires the recruitment of an unknown factor to the A-repeat of *Xist,* which is responsible for silencing. Yet, the factors directly interacting with *Xist* RNA are not known. Identifying new components of the inactive X chromosome holds promise for unravelling novel pathways for epigenetic gene silencing.

# Project 1: Investigation of the role of histone deacetylation in establishing a chromosomal memory during X inactivation

## Introduction

Previously, it has been shown that *Xist* expression during early differentiation regulated the efficiency recruitment of Saf-A and Ash2 as well as other proteins and modifications to the Xi in differentiated cells (Pullirsch 2008). Since continuous *Xist* expression was not required a memory had apparently been established on the chromosome at a specific time point, after 3 days of differentiation that could be maintained independent of *Xist.* However, neither Saf-A, Ash2 nor other proteins, which mark the Xi in differentiated cells, were maintained when *Xist* expression was turned off. This raised the question of the molecular basis for memory. Notably, establishment of memory has been observed independent of gene silencing, when recruitment of Polycomb complexes was used as readout (Leeb and Wutz, 2007; Schoeftner et al., 2006). This suggested that the mechanism of memory is different from the formation of a heterochromatic inactive X chromosome.

Global hypoacetylation of histone H4 had been previously shown to be established by *Xist* at the time of memory imposition independent of gene repression (Pullirsch et al., 2008) and was further maintained independent of *Xist*

on the silent Xi (Csankovszky et al., 1999; Pullirsch et al., 2008). Therefore, deacetylation of histone H4 represented a chromatin feature that correlated with memory and could be a component of its mechanism.

If histone H4 hypoacetylation were a critical component of memory, acetylation of histone H4 would be predicted to interfere with the recruitment of memory. Consequently, impaired memory could be readout by failure to recruit factors to the Xi. We attempted to test this prediction experimentally by blocking histone deacetylases using chemical inhibitors.

# Results

## Recruitment of Saf-A and Ash2 protein to the inactive X by *Xist* expression

In order to characterize the timing of Ash2 and Saf-A recruitment in X inactivation we used an inducible *Xist* expression system in mouse ES cells, which recapitulates the initiation and maintenance of chromosome-wide silencing (Wutz and Jaenisch, 2000). For this we used $\Delta sx^{SafA:hrGFP}$ male ES cells with an inducible promoter at the transcription start of the endogenous *Xist* gene, carrying a deletion of the 5´end including the so called repeat A and a Saf-A:hrGFP transgene (Wutz et al., 2002);(Pullirsch et al, 2008). *Xist* lacking repeat A localizes to the X chromosome, forms a compartment deficient in RNA polymerase II, recruits PcG proteins and establishes histone modifications (Chaumeil et al., 2006; Kohlmaier et al., 2004; Plath et al., 2003; Schoeftner et al., 2006). Expression of the mutant *Xist* RNA by addition of doxycycline does not result in gene repression avoiding thereby cell death due to inactivation of the single X chromosome of the male ES cells.

We induced differentiation with retinoic acid in $\Delta sx^{SafA:hrGFP}$ male ES cells and at the same time expression of *Xist* by doxycycline.

To determine the timing of Saf-A recruitment by *Xist* the number of hrGFP foci were counted during differentiation of $sx^{SafA:hrGFP}$ male ES cells. After 2 days of differentiation 10% of the cells showed focal SafA-hrGFP signals (Figure 4A). In contrast, we did not detect focal enrichment of the Saf-A-hrGFP protein after

induction of *Xist* expression in undifferentiated $\Delta sx^{SafA:hrGFP}$ ES cells. During further differentiation, the percentage of cells showing Saf-A foci increased to 48% between day 3 and 4. At the final time point (day 5) 65% of the cells showed focal Saf-A signals (Fig 4A).

In parallel cultures we detected Ash2 by immunofluorescence staining (Fig 4B). Ash2 recruitment was first observed on day 2 of differentiation with a significant rise in the number of cells showing Ash2 focal staining between day 3 and 4. This showed that recruitment of Ash2 obeyed similar kinetics as Saf-A.

Ash2 immunofluorescence staining of $\Delta sx^{SafA:hrGFP}$ ES cells was performed using a commercial antibody. In order to verify its specificity, we established 36.11. ES clones carrying a doxycycline inducible *Ash2L* RNAi construct and analyzed Ash2 protein levels and Ash2 recruitment upon doxycycline treatment (Figure 5). For this, 36.11 Ash2L RNAi clones 1 and 4 were differentiated with retinoic acid and RNAi was induced with doxycycline for 2 days. The effect of Ash2l RNAi was confirmed in two independent clones by Northern analysis (Figure 5B). A strong reduction of Ash2l transcript was observed after induction of RNAi by the addition of doxycycline. Western blot analysis showed a severe reduction of Ash2l protein in RNAi induced cells compared to control cells cultivated without doxycycline (Figure 5A). To further investigate Ash2l antibody specificity, Ash2l immunofluorescence staining was performed, which showed a clear reduction of cells containing Ash2l foci upon RNAi induction (Figure 5C). Since both immunofluorescence staining as well as western blot analysis showed a clear effect upon Ash2 RNAi induction, we conclude that the Ash2 antibody was specific.

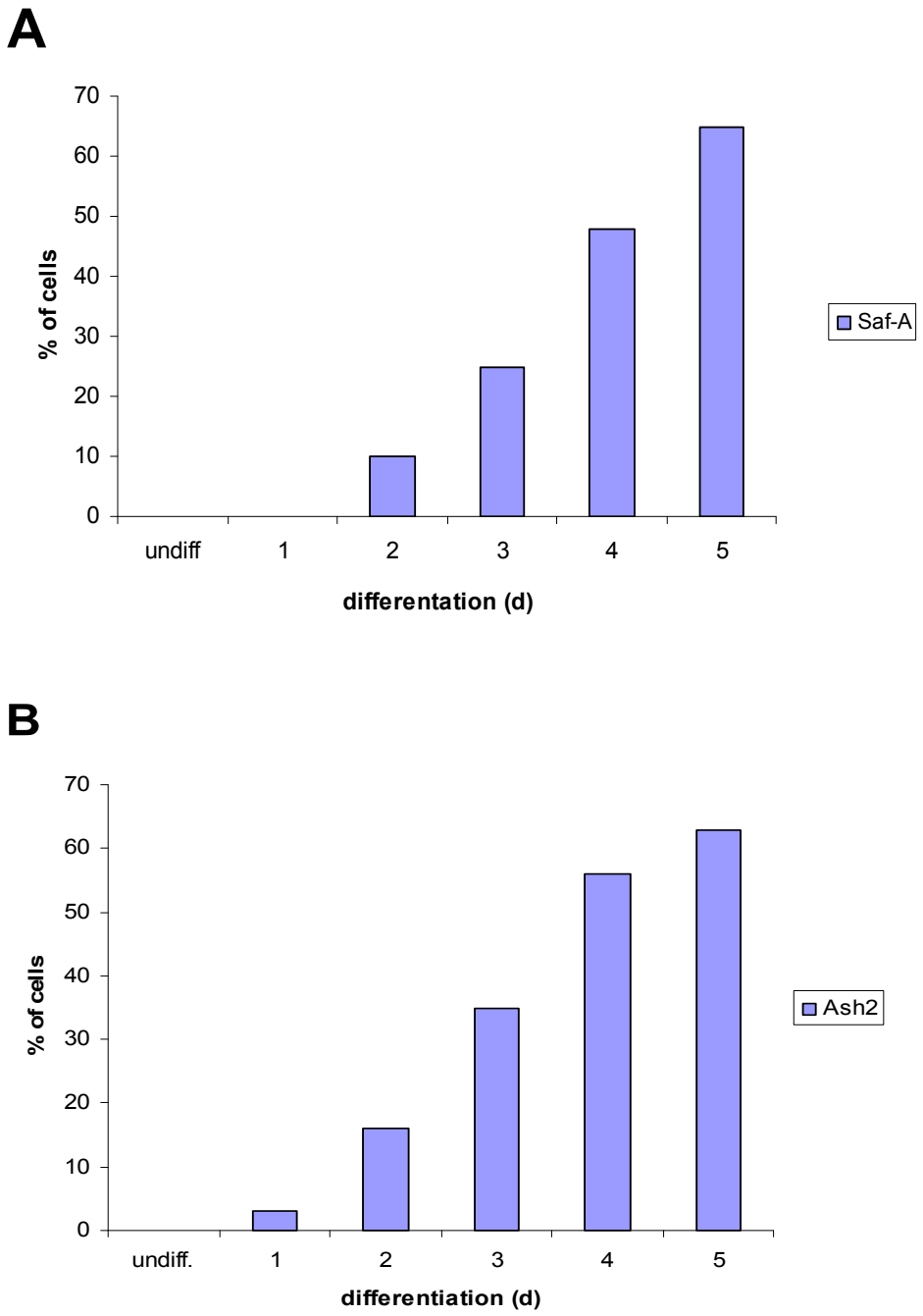


**Figure 4: Recruitment of Saf-A and Ash2 in $\Delta sx^{SafA:hrGFP}$ ES cells**

An analysis of Saf-A (A) and Ash2 (B) recruitment by *Xist* in undifferentiated $\Delta sx^{SafA:hrGFP}$ ES cells and after 1, 2, 3, 4 and 5 days of differentiation in the presence of doxycycline is shown. The percentage of cells showing focal enrichment is given (n=100).

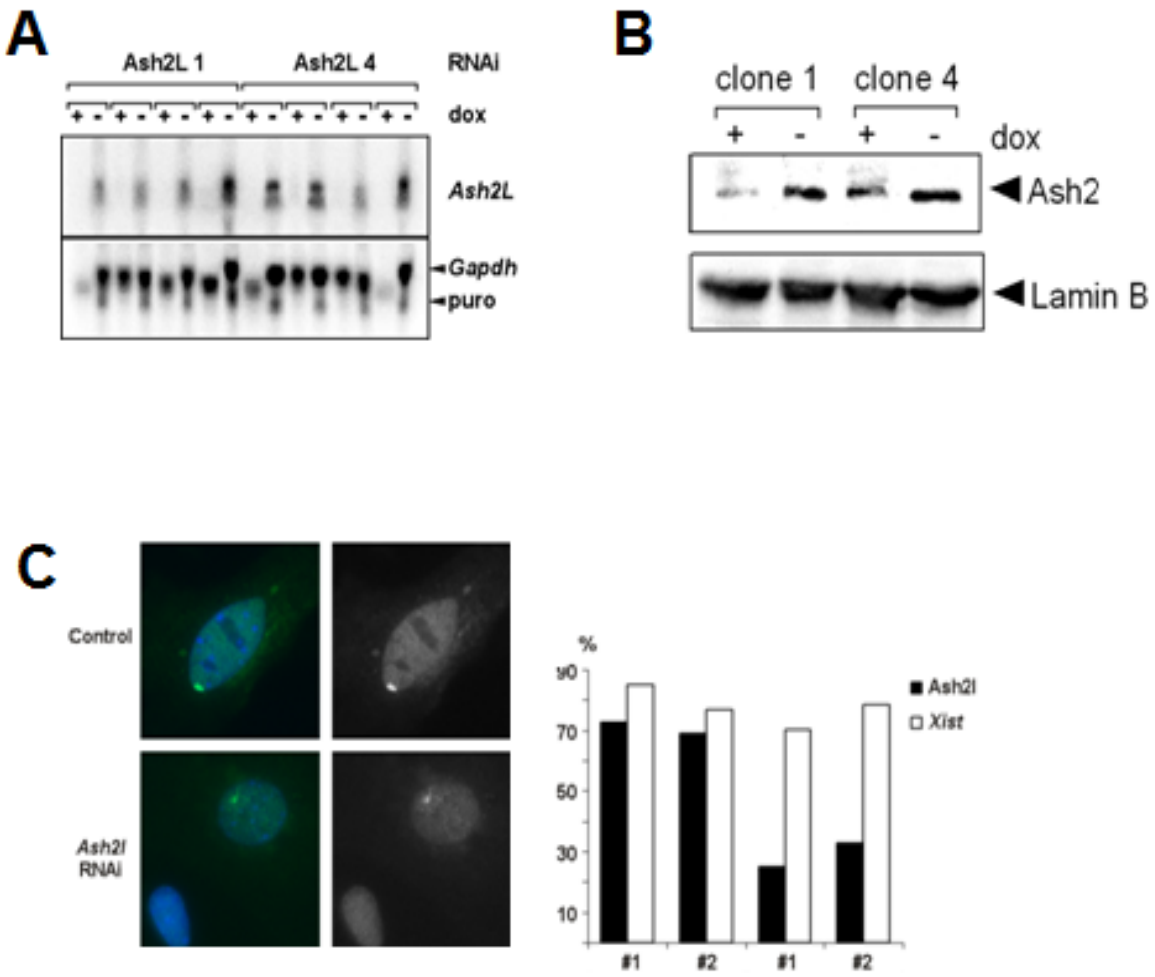


**Figure 5: Specificity of the Ash2l antibody staining of the Xi**

The effect of RNAi from 36 ES cells carrying inducible *Ash2l* RNAi constructs was confirmed by Northern analysis. Multiple clones are shown for two independent *Ash2l* constructs . Reduction of the Ash2l transcripts is observed upon induction of RNAi with doxycycline (+dox). *Gapdh* is a loading control. Puro is repressed by Xist induction with doxycycline in 36 ES cells (5A). Western analysis of Ash2l in extracts from 36 ES cells carrying inducible *Ash2l* RNAi constructs. Induction of RNAi by doxycycline (+dox) results in reduced amount of Ash2l protein (5B). Two independent RNAi constructs (#1 and #4) were analysed.. Immunofluorescence staining in differentiated 36 ES cells carrying inducible *Xist* and Ash2l RNAi constructs. Fewer and weaker Ash2l foci are observed in Ash2l RNAi clones compared to controls containing unrelated RNAi constructs (two independent constructs #1 and #2 are shown each). Statistical analysis of the number of cells showing Ash2l foci is given on the right. Ash2l RNAi does not affect *Xist* expression (5C).

## Reduction of cells containing Saf-A foci upon inhibition of sirtuins early in ES differentiation

For assessing the effect of histone deacetylase (HDAC) inhibitors on memory establishment $\Delta sx^{SafA:hrGFP}$ ES cells were differentiated for seven days with retinoic acid in the presence of doxycycline to induce *Xist* expression. Histone deacetylase inhibitors against class I, II and III of histone deacetylases were added from day 1 to day 5 of differentiation in parallel cultures. At day 7 of differentiation Saf-A recruitment and *Xist* localization were analyzed.

Control cultures were cultivated in the absence of inhibitors and served as a reference for memory recruitment. Induction of *Xist* late in differentiation, when memory cannot be recruited, served as a negative control (Figure 6).

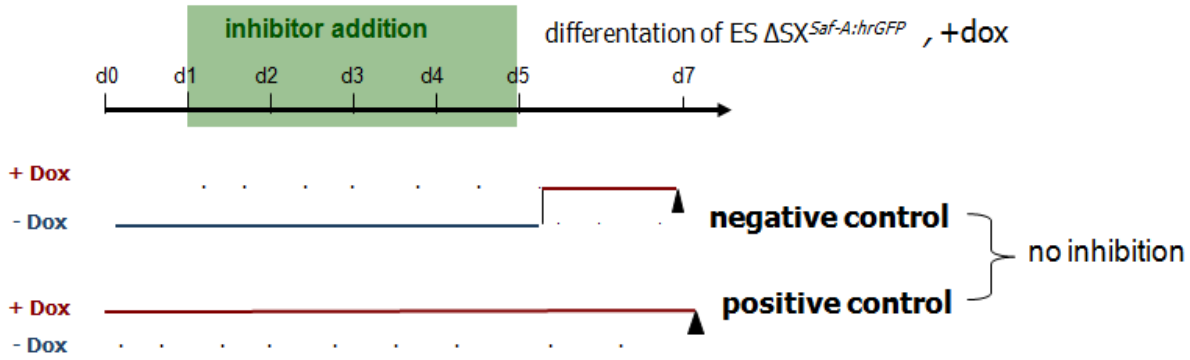


**Figure 6: Time course of the experimental setup**

Silencing deficient *Xist* was continuously induced in cultures treated from day 1 to day 5 with HDAC inhibitors. Both positive and negative controls were cultivated without inhibitors. *Xist* was induced throughout differentiation in the positive control and from day 5 on in the negative control.

As expected positive as well as negative control cells show *Xist* localization in the vast majority of cells. Since *Xist* was not induced during memory formation in the negative control, the recruitment of the Saf-A protein, which is dependent on memory, is severely reduced compared to the positive control.

TSA and MS275 treated cells show a severe reduction of cells containing Saf-A foci. However, indirect effects due to inhibition of deacetylases could not be ruled out as disperse *Xist* clusters were observed, suggesting that these HDAC inhibitors had led to delocalization of *Xist* (Figure 7).

To further investigate whether DNA methylation could play a role in memory formation, we included RG108, a DNA methylation inhibitor, in our study. Addition of RG108 during the first 5 days of differention of $\Delta sx^{SafA:hrGFP}$ ES cells had no effect on the number of cells showing Saf-A foci compared to controls. This suggests that DNA methylation is not critical for memory formation (Figure7).

Inhibition of sirtuins using Sirtinol, which is a specific HDAC class III inhibitor, shows a severe reduction in the number of cells containing Saf-A recruitment and very little effect on *Xist* localization. *Xist* clusters were similar in appearance compared to the controls (Figure 7, 8). These results strongly suggest HDAC class III to be involved in the establishment of chromosomal memory.

For further verification, we analysed the effect of HDAC inhibition on endogenously expressed Ash2 protein. For this, ES $\Delta sx^{SafA:hrGFP}$ were differentiated for seven days in the presence of retinoic acid. 100mM Sirtinol and 2µM MS275 were added from day 1 to day 5, treating the cells in parallel

cultures. At day 7 of differentiation Ash2 and Saf-A recruitment as well as *Xist* localization were analyzed. Controls were cultivated in the absence of inhibitors. Xist was induced throughout differentiation in the positive control and after the timepoint for memory formation in the negative control (Figure 6).

As expected, positive as well as negative controls showed *Xist* localization in the vast majority of cells (Figure 9A). Since *Xist* was not induced during memory formation in the negative control, the recruitments of Saf-A as well as Ash2 protein, which are both dependent on memory, is severely reduced compared to the positive control (Figure 9A and 9B).

MS275 treated cells show a severe reduction of cells containing Saf-A foci, but Ash2 recruitment was unaffected. Again, disperse *Xist* clusters were observed, which lead to the assumption that these HDAC inhibitors had led to delocalization of *Xist*.

Sirtinol treatment caused a clear reduction of cells containing Ash2 as well as Saf-A foci whereas Xist localization was unaffected.

Since the recruitment of Saf-A as well as Ash2 protein, which are both dependent on memory, strongly decreases upon inhibition of sirtuins, we speculate that histone H4 Lysine 16 hypoacetylation is a critical component of memory.

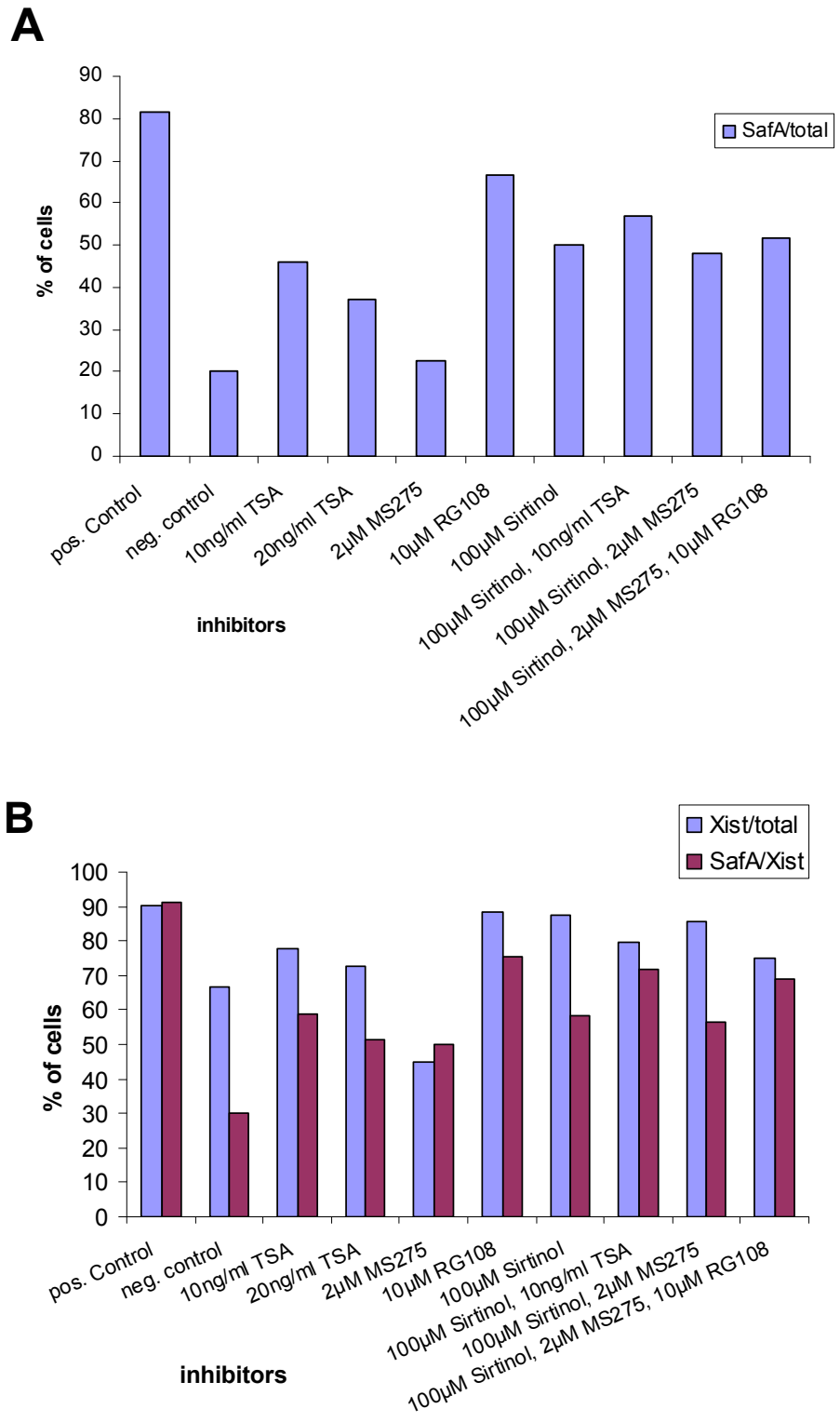


**Figure 7: Reduction of Saf-A recruitment upon early HDAC inhibition in ES $\Delta sx^{SafA:hrGFP}$**

Doxycycline and inhibitors were added at time points during differentiation listed in Figure 2. The percentage of cells showing Saf-A ( A) and Xist (B) recruitment is plotted (n=100).

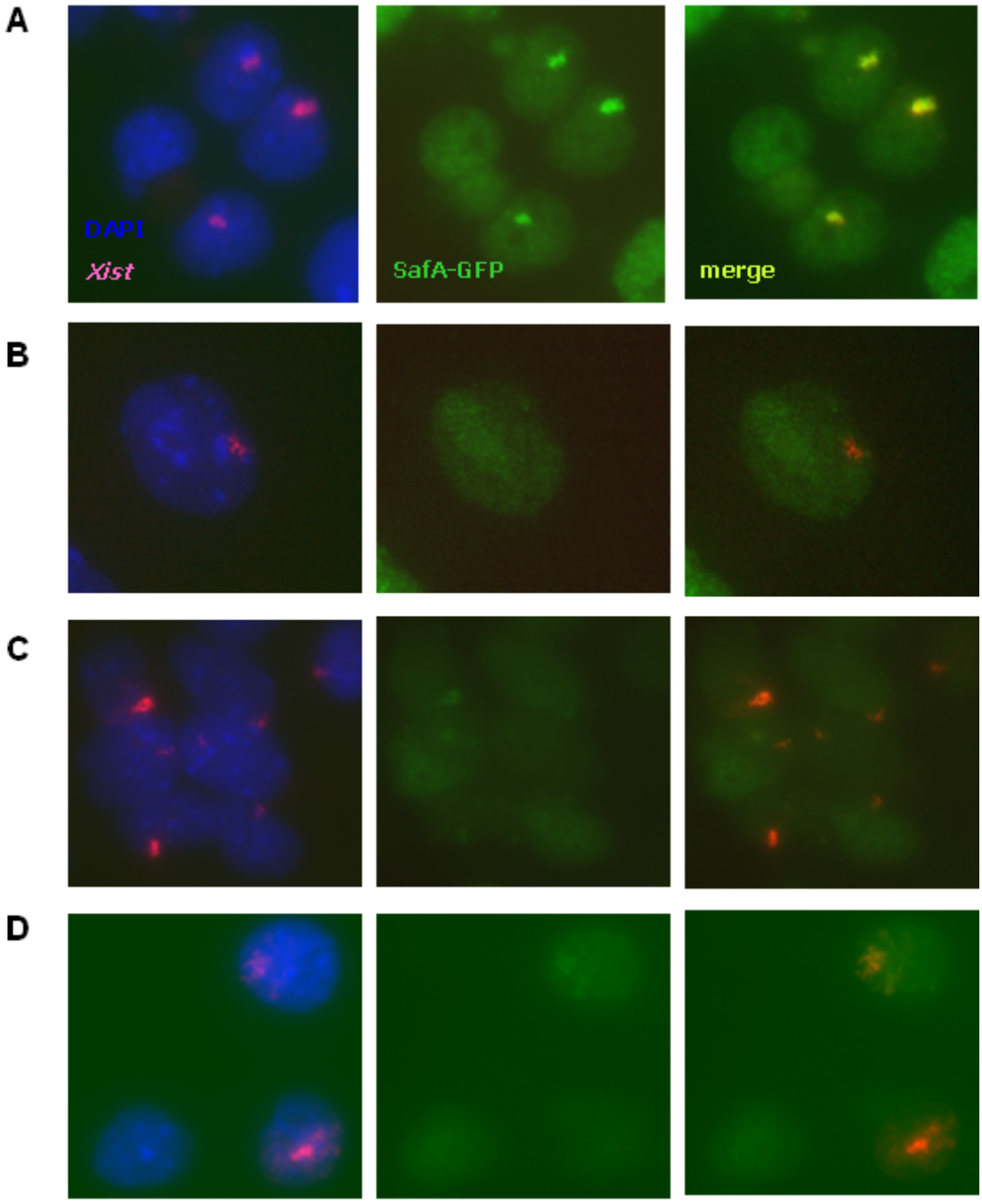


**Figure 8: Inhibition of HDAC class II and III early in ES differentiation**

*Xist* RNA FISH and Saf-A-GFP of positive (A) and negative (B) control cultures as well as 100mM sirtinol (C) and 2µM MS275 (D) treated cells. *Xist* clusters remain similar in appearance upon sirtinol treatment (C), upon MS275 disperse *Xist* clusters were observed.

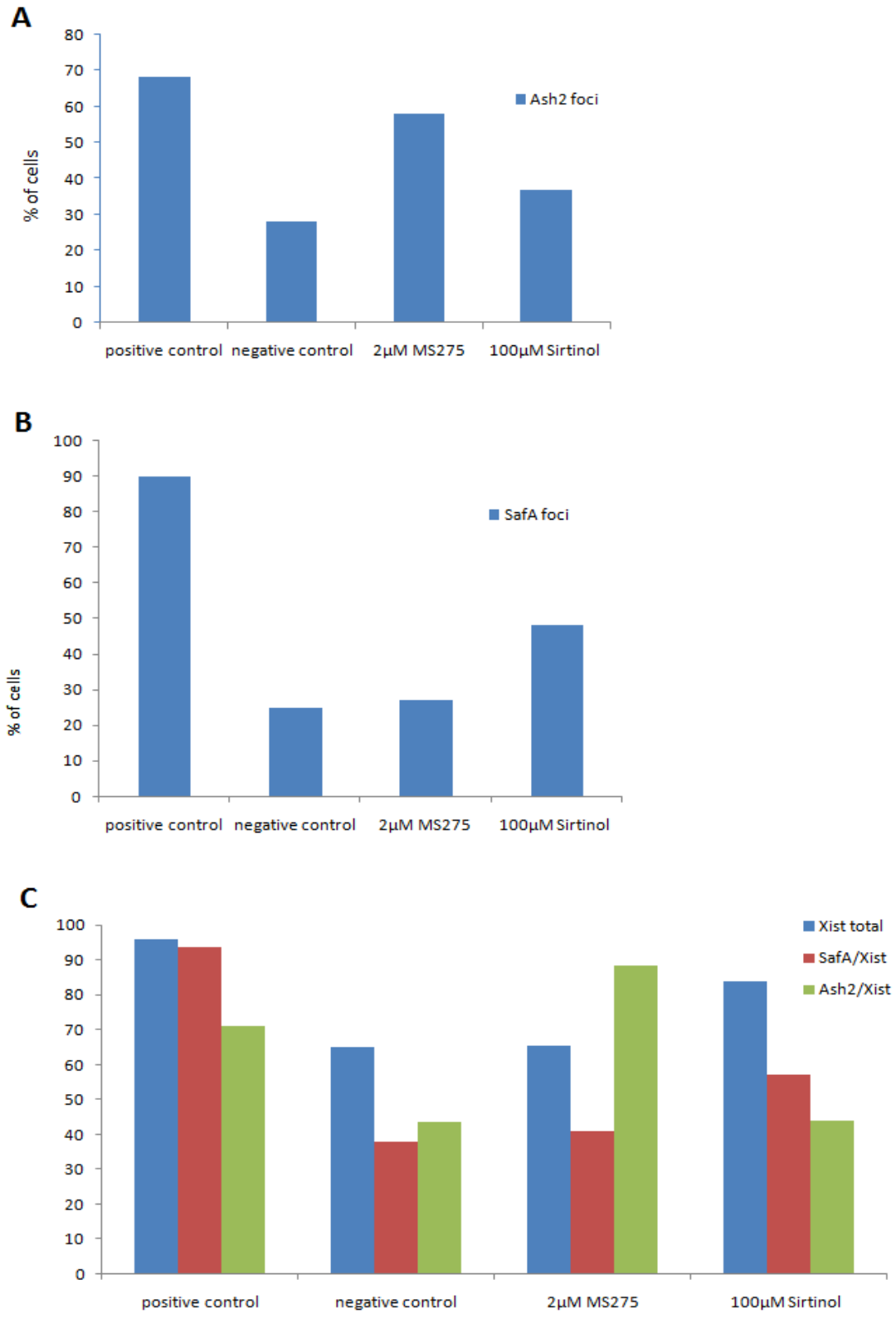


**Figure 9: Recruitment of Ash2 and SafA upon inhibition of HDAC class II and III**

Doxycycline and inhibitors were added at time points during differentiation listed in Figure 2. The percentage of cells showing Ash2 (A), Saf-A (B ) and Xist (C) recruitment is plotted (n=100).

## Investigation of sirtuin localization

Consistent with the idea that sirtuins act in memory establishment treatment with Sirtinol, a specific HDAC class III inhibitor, early during differentiation interferes with Saf-A and Ash2 recruitment to the Xi.

Mammals possess seven sirtuins (SIRT1-7) that occupy different subcellular compartments such as the nucleus (SIRT1, -2, -6, -7), cytoplasm (SIRT1 and SIRT2) and the mitochondria (SIRT3, -4 and -5).

To verify the importance of sirtuins in the process of X chromosome inactivation, we investigated the localization of sirtuins.

Therefore we performed immunofluorescence staining testing six different commercial SIRT1 and two different SIRT2 antibodies on 293-SafA-GFP as well as X3-SafA-GFP cells. These cell lines contain three X chromosomes; two of them, marked by the recruitment of SafA-GFP protein, are inactive.

Immunofluorescence staining for SIRT2 showed cytoplasmic localization in both X3-SafA-GFP as well as 293-SafA-GFP cells (Figure 7A and 7C). Sirt1 was located in the nucleus, but did not show co localization with the SafA-GFP signal (Figure 7B).

We did not observe co-localization of sirtuins with the inactive X chromosome. Therefore, recruitment of Sirtuins to the Xi remains to be shown. Nevertheless, our data do not rule out that such recruitment takes place. There are technical limitations due to antibody quality that could have prevented us from detecting sirtuis at the Xi. Alternatively, sirtuins could be recruited transiently to the Xi at a specific interval in differentiation or at a low amount such that

detection could be difficult. It cannot be ruled out that other Sirtuins than Sirt1 and Sirt2, for which we had antisera available, are involved. Further studies will be required to fully address this issue.

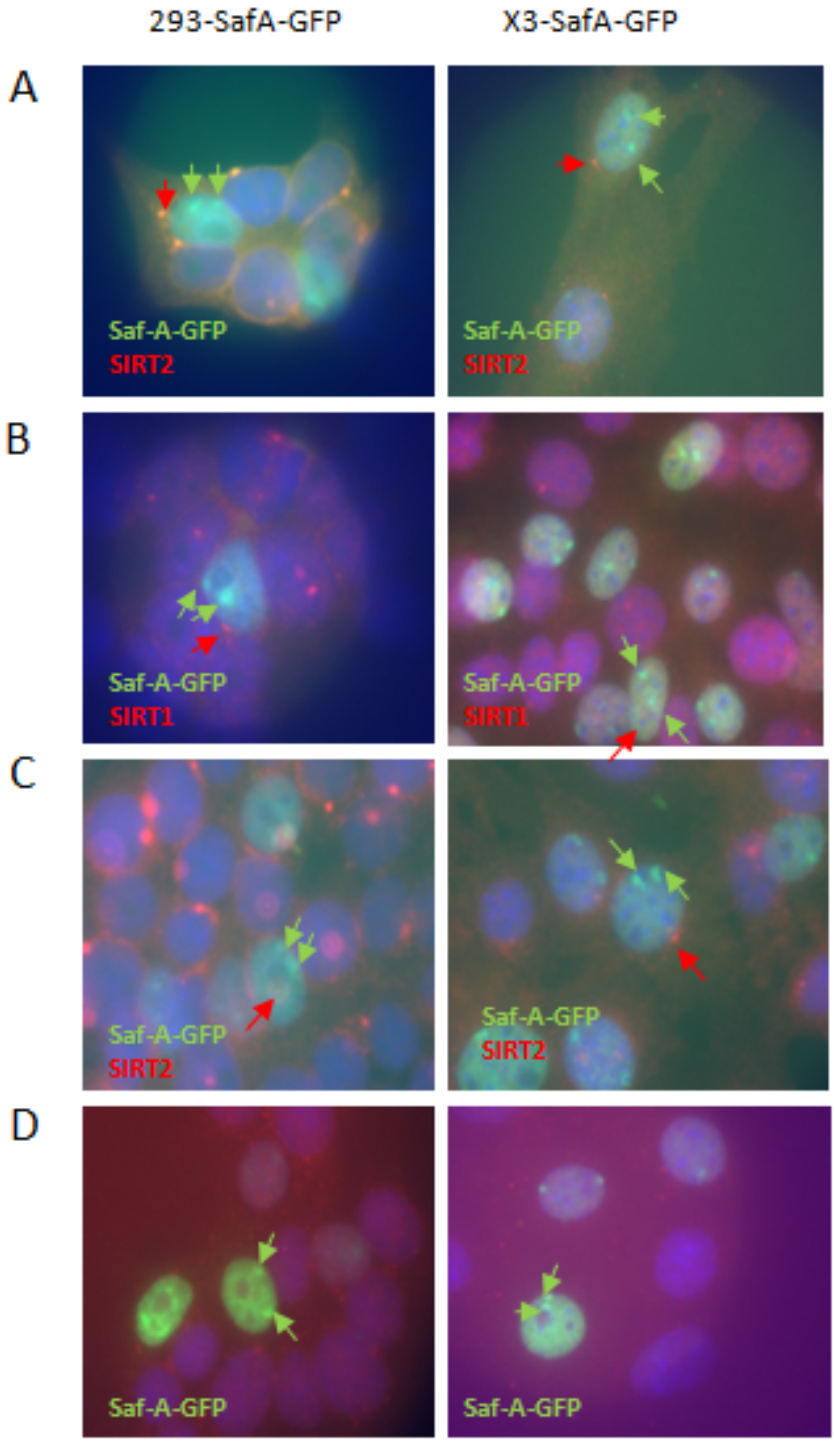


**Figure 10:**

**Localization of sirtuins**

SIRT1 and SIRT2 immunofluorescence staining was performed using 293-SafA-GFP and X3-Saf-A-GFP cells, which display two SafA-GFP marked inactive X chromosomes.

SIRT2 staining showed cytoplasmic localization. SIRT2 staining using gene tex antibody is illustrated in Figure 10A and SIRT2 antibody from Santa Cruz in Figure 10C. SIRT1 (abcam) showed nuclear localization but no co localization with Saf-A was observed (B).

# Discussion

The chromosomal memory is a chromatin feature on the X chromosome, which is established by *Xist* at a specific timepoint in early ES cell differentiation. The molecular basis of this chromosomal change is presently unknown.

Deacetylation of histone H4 represents a chromatin feature that correlated with memory and could be a component of its mechanism. Thus, we investigated histone H4 deacetylation as a critical component of the chromosomal memory. We predicted that acetylated histone H4 would interfere with the recruitment of memory. Hence, we tested this prediction by blocking histone deacetylases. Among different HDAC inhibitors we identified Sirtinol as a specific class III inhibitor that potentially can block memory formation. We show that Saf-A and Ash2 recruitment by *Xist* are impaired when ES cells are differentiated in the presence of Sirtinol. *Xist* localization is not affected under these conditions suggesting a defect in chromatin features required for memory. It remains to be shown how inhibition of class III HDACs interferes with memory formation and if this is a direct effect. In the simplest case it can be envisioned that Sirtuins are recruited by *Xist* to the Xi, where they catalyze deacetylation H4. We have tested this hypothesis by immunofluorescence analysis using antisera specific for SirT1 and SirT2. In these studies we did not observe co-localization of SirT1 and SirT2 with the inactive X chromosome. Thus, these results do not support our hypothesis that Sirtuins are recruited by *Xist*. However, there are several limitations to this interpretation. In principle, the commercial antisera that were accessible to us could potentially not be suitable to detect Sirtuins at the Xi.

Albeit, this is unlikely as we have used several independent sera, detection could be difficult if Sirtuins were transiently recruited or in a low amount. We cannot rule out the possibility that members of the SirT family other than SirT1/2 are recruited specifically to the Xi. Thus, our failure to detect Sirtuin recruitment by *Xist* does not rule out a direct involvement of class III HDACs in memory formation.

Future work is needed to elucidate the mechanism of Sirtuin action in X inactivation. It will be important to genetically follow up the role of individual SirT family HDACs in X inactivation. Approaches using gene targeting or RNAi in ES cells will be useful to this end. Furthermore, it has to be clarified what effect deacetylation of H4 lysine 16 has on memory imposition. The deacetylation reaction produces an unusual metabolite O-acetyl-ADP ribose that has been shown in yeast to trigger a change in chromatin structure. It will be interesting to see if a similar mechanism is also operative at memory formation during X inactivation. Studies into the establishment of heritable epigenetic states in mammals are important for questions such as cell identity and gene expression control. Thus, unraveling the pathway leading to memory formation in X inactivation has important implications for stem cell differentiation and disease. Recently, more and more components of the maintenance machinery for the Xi are identified such as SmcHD1 (Blewitt et al., 2008). Thus, future research promises interesting insights into the underlying molecular mechanism.

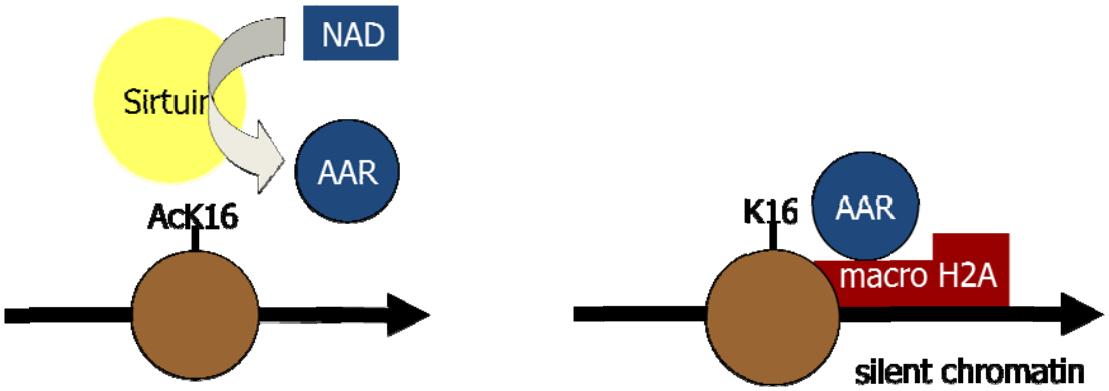


**Figure 11: Hypothesis of sirtuin mediated histone H4 hypoacetylation and macro H2A recruitment to the X chromosome**

Sirtuins deacetylate lysine 16 of histone H4 in an NAD dependent reaction leading to the production of AAR. AAR has been shown to bind to macroH2A via the non-histone domain. I hypothesize that AAR bound macroH2A is cooperatively recruited to chromatin and accumulates on the inactive X chromosome. This idea is derived from the yeast Sir3 protein, which undergoes conformational change upon AAR binding and cooperatively binds to the silent mating type loci for gene repression.

# Project 2: A biochemical approach for the identification of factors involved in the initiation of mammalian X chromosome inactivation

## Introduction

The development of an inducible *Xist* expression system in male ES cells made it possible to experimentally control the initiation of chromosome-wide silencing in ES cell differentiation. Investigations using this system showed that chromosomal silencing is a two step process. During the initiation phase of X inactivation, *Xist* causes efficient, but reversible gene silencing (Wutz and Jaenisch 2000). Yet, after 72 hrs of differentiation *Xist* is no longer required for maintenance of the inactive state (Csankovszki et al., 1999). Taken together these studies strongly suggest that early reversible silencing initiates XCI. Upon differentiation a transition to a chromatin state occurs that establishes irreversible gene silencing and maintenance of XCI (Wutz and Jaenisch 2000).

In somatic cells, gene repression on the Xi is maintained by several epigenetic mechanisms. Factors that have been implicated in the maintenance of X inactivation include DNA methylation, late chromosomal replication and histone H4 hypoacetylation (Csankovszki et al., 2001; Csankovszki et al., 1999; Keohane et al., 1996; Sado et al., 2000).

The earliest event in X inactivation is an exclusion of the transcription machinery from the Xi chromosome territory. RNA polymerase II, splicing factors and nascent transcripts are absent from the *Xist* covered chromosome. However, the formation of this *Xist* covered chromosome territory is not sufficient for gene repression. Initiation of silencing depends on the 5´-end of *Xist* RNA and a specific cellular context that is presented by cells of the early embryo (Savarese et al., 2006; Wutz et al., 2002). Thus far, factors that cooperate with *Xist* the initiation of chromosome-wide silencing have not been identified.

In order to identify candidates for factors involved in the initiation of X chromosome inactivation, we aimed at the biochemical isolation of the *Xist* containing complexes from ES cells. For this we devised a protocol to isolate the nuclear fraction in which *Xist* is contained and to detect proteins that become enriched upon X inactivation.

## Experimental strategy

To identify candidate proteins that interact with *Xist* RNA we aimed to compare ES cells with an inactive X chromosome to ES cells with an active X chromosome. In our experimental design, we used ES cells which have an inducible *Xist* allele on the X chromosome such that inactivation can be triggered by addition of doxycycline to the growth medium (Figure 11).

*Xist* RNA has been observed to remain in the nuclear matrix. This suggests that a specific nuclear fraction that is enriched for *Xist* RNA can be isolated.

Therefore, we focused our biochemical purification on the nuclear fraction that contains *Xist*. Importantly, this would remove chromatin from nuclei by DNA digestion and protein salt extraction effectively eliminating bulk histones and other abundant nuclear factors. We reasoned that we subsequent might be able to specifically extract candidate proteins from this fraction by digestion *Xist* RNA. Proteins becoming soluble after RNA digestion can be analysed by mass spectrometry.

Analysis of complex protein mixtures has become possible due to recent developments in mass spectrometric methodology (REFs: Mathias Mann review; Mann and Schoeler Hans 5000 proteins in ES cells by SILAC). Comparison of protein fractions between two samples requires a quantitative approach to proteomics. This can be achieved in a first approximation by integration of peak areas of mass spectra. Precise quantification requires methods for labelling the peptides with different masses. This can be achieved by incorporation of isotopic aminoacids. One sample is labelled with light amino acids and compared to cells labelled with amino acids containing heavy nitrogen and carbon isotopes ($^{15}N$ and $^{13}C$).

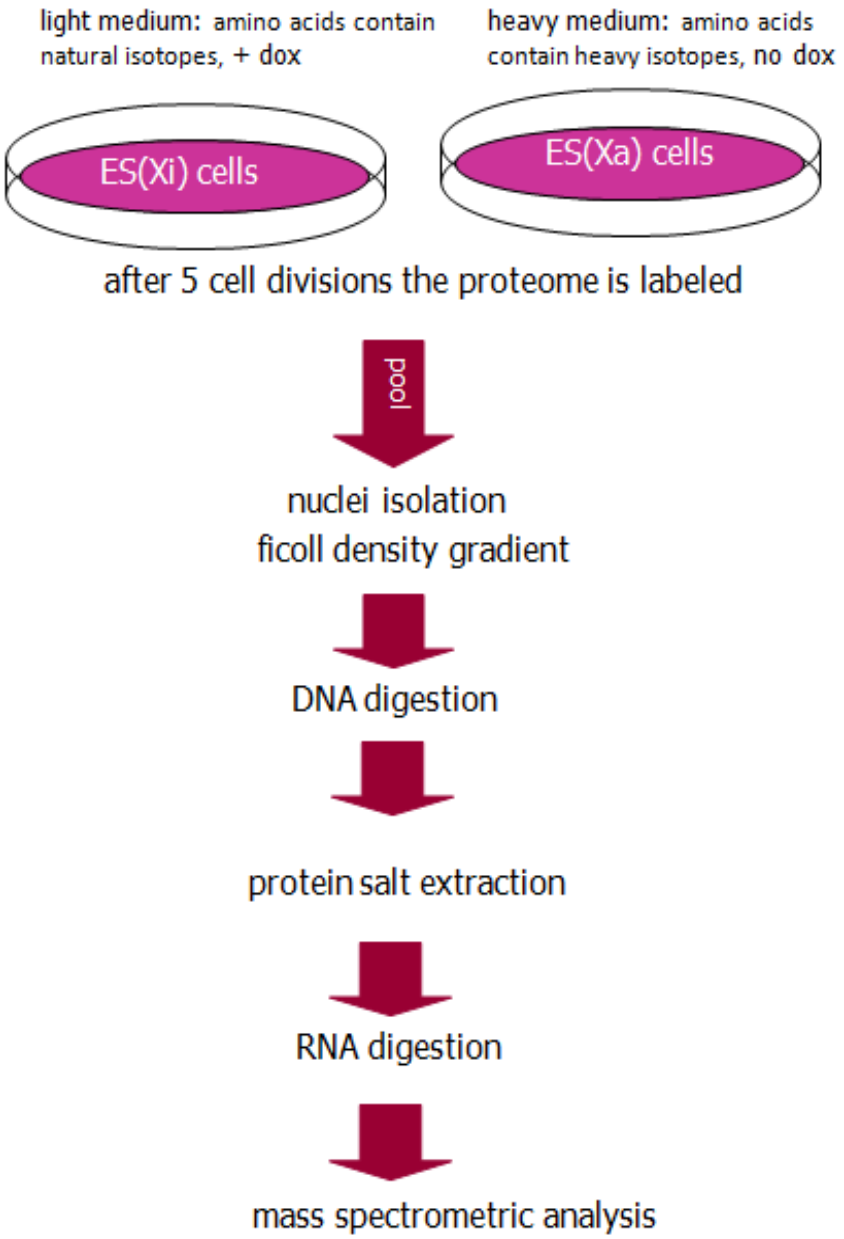


**Figure 12: Experimental design to compare protein levels of ES (Xi) to ES (Xa)**

ES cells with an inactive X are labelled with light amino acids and ES cells with an active X with heavy amino acids. Subsequently, chromatin is removed from nuclei by DNA digestion and protein salt extraction. The remaining *Xist* containing fraction is isolated. Proteins becoming soluble after RNA digestion are analysed by mass spectrometry.

# Results

## *Xist* RNA remains in fixed nuclear matrix fraction of ES cells

Earlier studies in female human epithelial cells have shown that *XIST* RNA remains in the nuclear matrix fraction. After DNA digestion and chromatin extraction *XIST* was detected by RNA fluorescence hybridization (Clemson et al., 1996). We adopted this strategy for optimization of extraction of the *Xist* containing nuclear fraction from ES cells using glass slides.

To investigate the efficiency of different DNA digesting enzymes, $\Delta sx^{SafA:hrGFP}$ ES cells were grown on multiwell glass slides (Roboz slides), washed in cytoskeletal buffer and salt extracted. DNA was either digested with DNAse I or PstI and HaeIII. Preparations treated with PstI and HaeIII showed intense DNA staining suggesting inefficient removal of chromatin. In contrast, cells treated with 10U/100µl DNAse I showed minimal residual DNA staining (data not shown). Thus, DNAse allowed effective removal of chromatin and was suitable for our purification scheme.

To investigate whether *Xist* RNA is retained after removal of bulk chromatin, biochemical fractionation procedures were examined that have been previously used to isolate insoluble nuclear fractions termed matrix and that remove 90-95 % of cellular DNA, proteins and phospholipids (Berezney and Coffey, 1974).

For this, $\Delta sx^{SafA:hrGFP}$ ES cells were used that contain an inducible *Xist* allele on the X chromosome, which lacks the 5´-end and does not trigger gene silencing.

In addition these cells contain a transgene for expression of a Saf-A:hrGFP fusion protein. *Xist* was induced for 24 hours by addition of doxycycline to the culture. Cell fractionation was performed in the following steps.

After cells were washed in PBS, preextraction with cytoskeletal buffer was performed. Chromatin was removed using ammonium sulphate extraction and DNA digestion using 10U/100µl DNAse I. A second extraction with ammonium sulphate was performed. The presence of *Xist* RNA was analysed using fluorescence *in situ* hybridization (FISH) after each fractionation step. Samples before fractionation as well as samples which were preextracted with cytoskeletal buffer, showed distinct *Xist* clusters. However, *Xist* did not remain in the insoluble fraction after treating the cells with ammonium sulphate. Minimal residual DNA staining was observed after DNA digestion and salt extraction (Figure 13).

These data indicate that *Xist* RNA is not retained after stringent extraction of the nuclear matrix suggesting that *Xist* binding was not stable in ES cells. *Xist* stability might have been compromised due to lack of the repeat A of *Xist* in $\Delta sx^{SafA:hrGFP}$ ES cells or short *Xist* induction time.

To circumvent these stability problems, the experiment was repeated in mouse ES cells which carry an inducible *Xist* cDNA transgene, which includes the repeat A, inserted into chromosome 11 (Wutz and Jaenisch, 2000). Induction of transgenic *Xist* recapitulates all known chromatin changes of X inactivation and causes silencing of the autosome.

*Xist* was induced for 3 days by doxycycline. Subsequently, cell extraction was performed as described above. Additionally, the effect of higher amounts of DNAse I for more efficient DNA digestion was investigated. We compared treatment with 10U/100µl to treatment with 100U/100µl. Residual DNA staining of

both samples did not show any difference; indicating that 10U of DNAse is already a sufficient for complete digestion of chromatin. Analysis of the samples by FISH showed that *Xist* RNA was not retained after extraction of the cells with ammonium sulphate (Figure 14).

Hence, both $\Delta sx^{SafA:hrGFP}$ ES as well as 36.11 ES cells showed *Xist* loss after extracting the cells with ammonium sulphate. We conclude from these data that *Xist* does not retain in the nuclear matrix of undifferentiated ES cells.

In order to stabilize *Xist* in the nuclear matrix fraction of ES cells we aim to enhance *Xist* binding to the matrix. Sodium tetrathionate is known to stabilize selectively nuclear matrix proteins by oxidizing sulfhydryl groups to disulfides. We anticipated that fixing ES cells with sodium tetrathionate leads to better preservation of nuclear matrix and thus might retain *Xist* RNA.

36.11 ES cells were cultivated in the presence of doxycycline for 3 days. Cells were preextracted in the presence of 2mM sodium tetrathionate and nuclear matrix extraction was performed as described above. *Xist* fluorescence *in situ* hybridization showed *Xist* RNA to remain after extracting the cells with ammonium sulphate as well as after whole fractionation procedure (Figure 15).

Thus, mild fixation with tetrathionate allowed me to devise a procedure that leads to the retention of *Xist* RNA in a partially purified nuclear matrix fraction of undifferentiated ES cells.

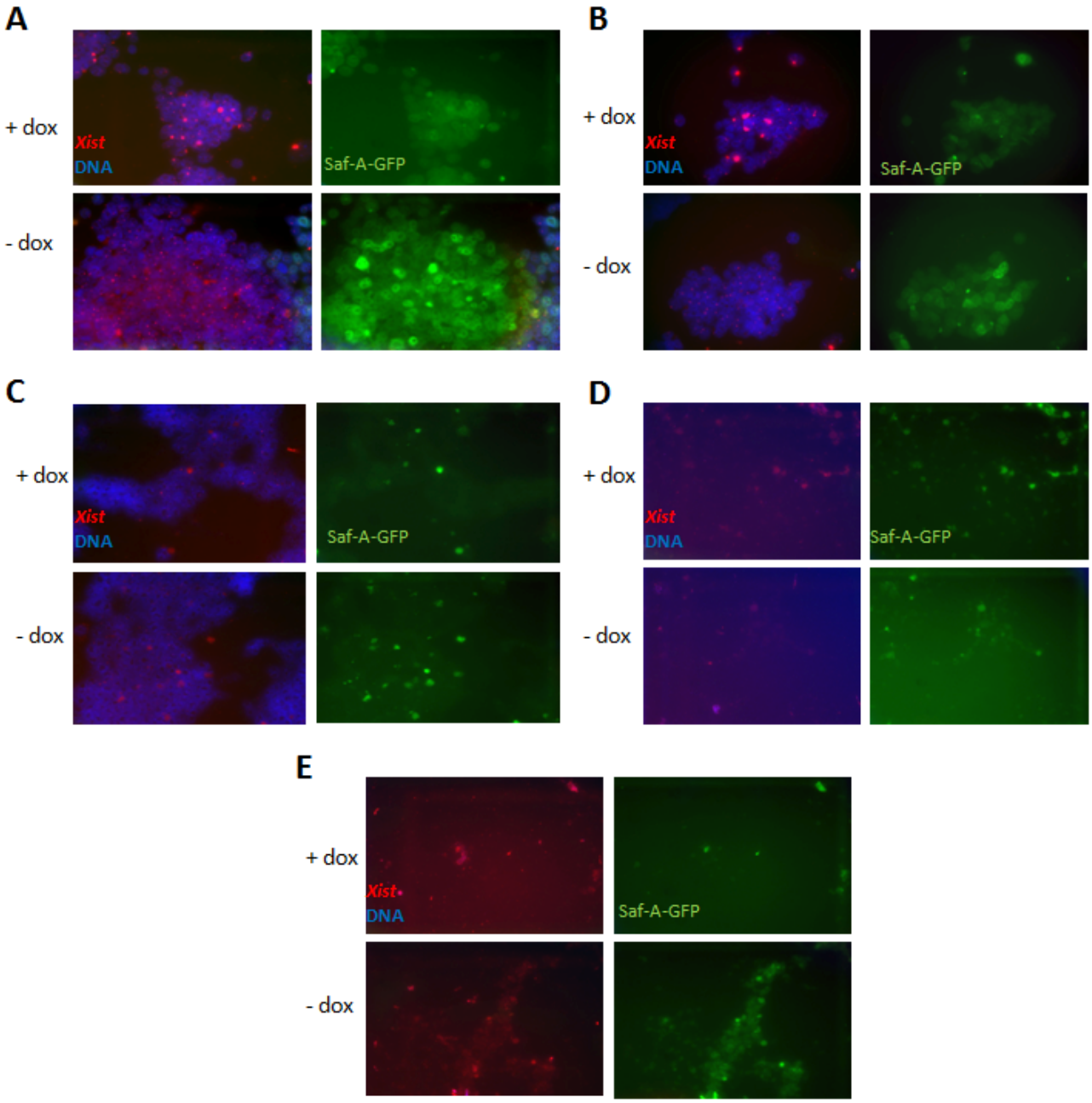


**Figure 13: *Xist* fluorescence *in situ* hybridization of fractionated ES $\Delta sx^{SafA:hrGFP}$ cells**

ES cells were preextracted with cytoskeletal buffer (B) and salt extracted with ammonium sulphate C). After DNA digestion (D), cells were again salt extracted (E). Samples before fractionation are shown (A). DNA was stained with DAPI. SAF-A is a nuclear matrix component of the Xi in differentiated cells but not of ES cells.

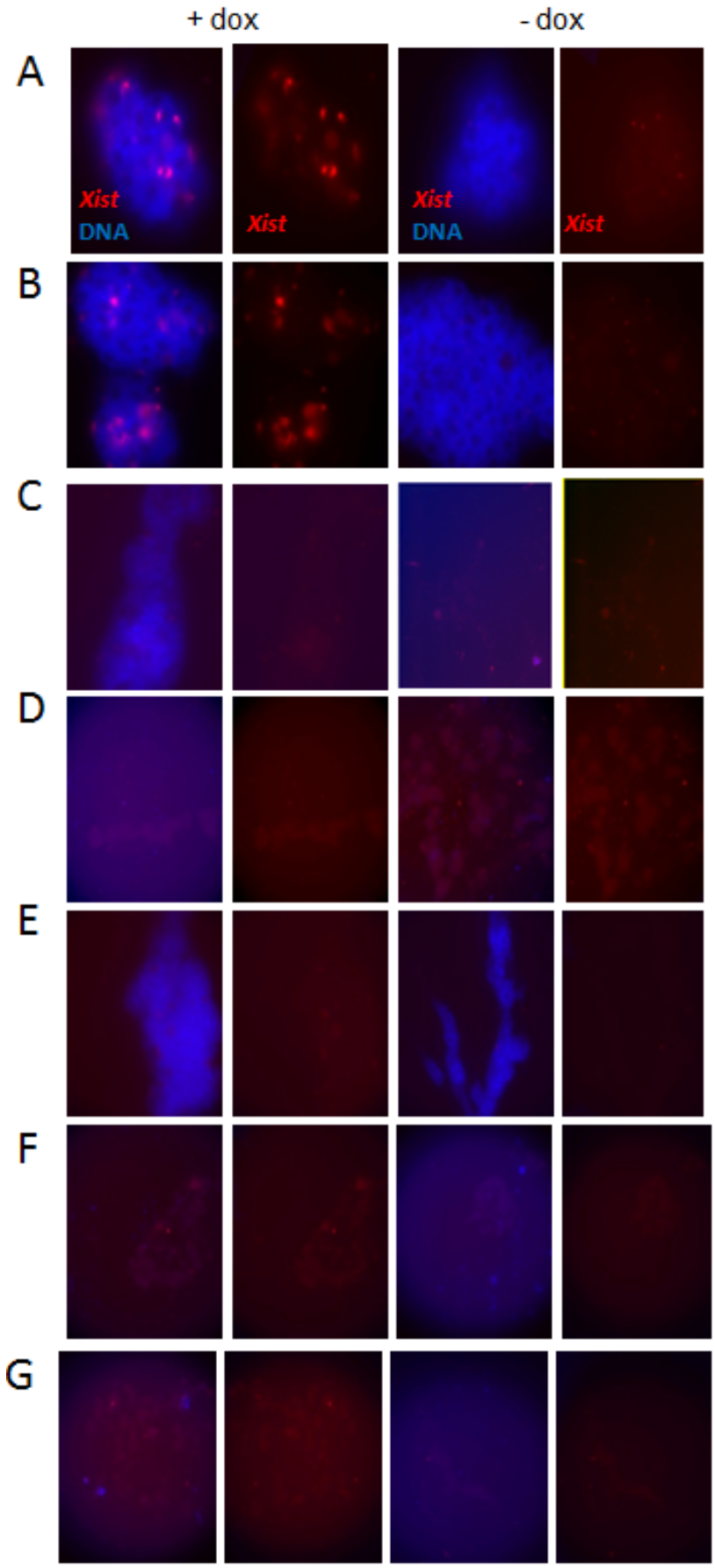


**Figure 14: *Xist* fluorescence *in situ* hybridization of chromatin extracted 36.11 ES cells**

ES cells were preextracted with cytoskeletal buffer (B) and salt extracted with ammonium sulphate (C). After DNA digestion (10U/100µl) (D), cells were again salt extracted (F and G). DNA was digested using 10U/100µl (F) or 100U/100µl DNAse I (G). Samples before nuclear extraction are shown (A). DNA was stained with DAPI.

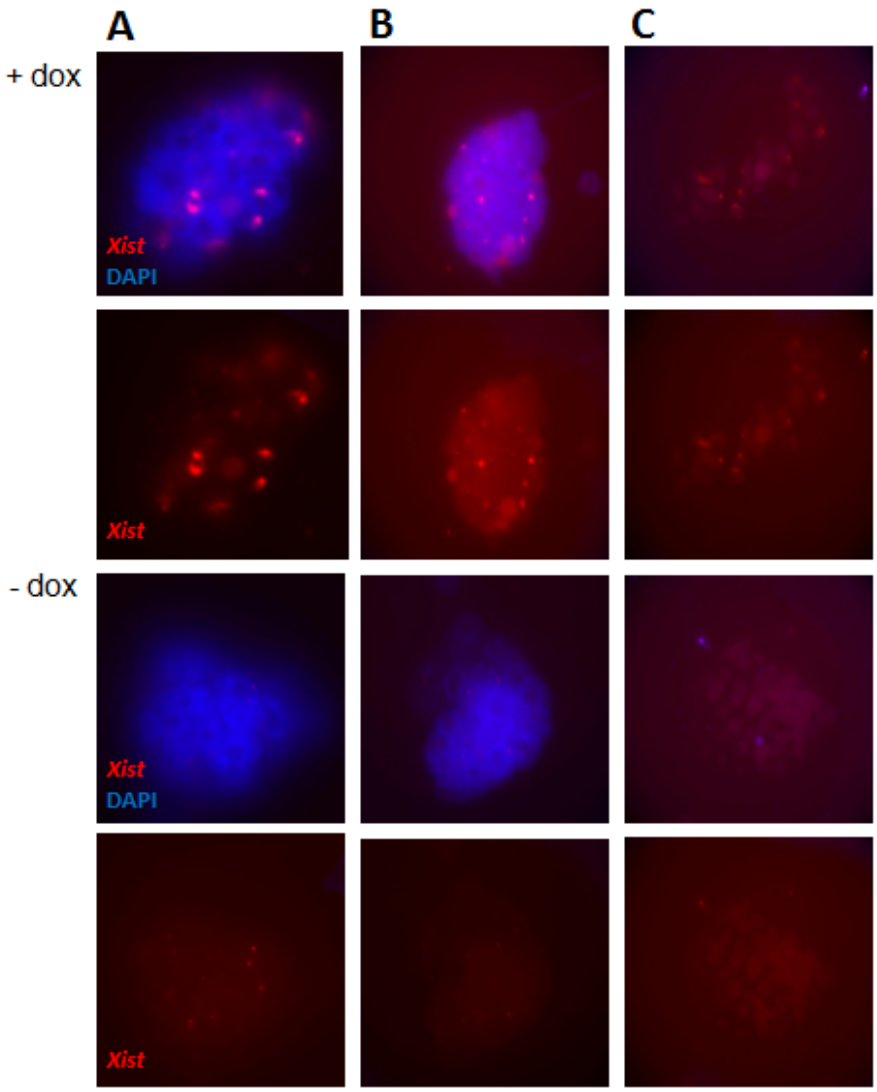


**Figure 15: *Xist* fluorescence *in situ* hybridization of 36.11 ES cells extracted cells using sodium tetrathionate**

ES cells were preextracted with cytobuffer in the presence of 2mM sodium tetrathionate and salt extracted with ammonium sulphate (B). After DNA digestion (10U/100µl), cells were again salt extracted (C). Samples before fractionation procedure is shown (A). DNA was stained with DAPI.

## Optimization of biochemical ES cell fractionation

For large scale preparative isolation of nuclear fractions containing *Xist* the optimized procedure from glass slides was adopted for a biochemical approach. For this nuclei were isolated from ES cells and fractionation steps to obtain a nuclear fraction suitable for detection of factors involved in the initiation phase of X chromosome inactivation were optimized. 36.11 ES cells were cultivated in the presence of doxycycline for 2 days to induce *Xist* expression. After harvesting the cells by trypsinization, nuclei were isolated to remove the cytoplasm. Subsequently, chromatin was removed by ammonium sulphate extraction and DNA digestion using 10U/100µl DNAse I. A second extraction with ammonium sulphate was performed to remove the digested chromatin. From the residual fraction proteins were then solubilised by RNAse treatment and analysed.

In order to obtain relatively pure and defined fractions we optimized several steps of this protocol. We attempted to isolate nuclei from ES cells using a Dounce glass homogenizer with loose fitting pestle. Following homogenization**,** nuclei were separated through a sucrose cushion. This protocol gave a viscous and ill defined pellet indicating nuclear lysis. Since nuclei were not intact and leaking DNA led to extreme viscosity subsequent treatment with ammonium sulphate and DNAse did not resolve the pellet. Therefore, chromatin could not be extracted from this preparation and an alternative protocol had to be envisioned. The destruction of the nuclei might have resulted from using a hypotonic sucrose gradient or from too strong shearing during homogenization.

Hence, we aimed to isolate intact nuclei, using a ficoll gradient, instead of sucrose gradient, which contains NP-40 and Triton. This method allows performing the destruction of the cell membrane and harvesting of nuclei by density gradient in one step.

ES cells were overlaid onto a cushion containing ficoll, NP-40 and Triton. Subsequent centrifugation separated nuclei from cytoplasm. We obtained intact nuclei suitable for our fractionation procedure.

Yet, we observed that DNA was not digestible after ammonium sulphate salt extraction. Therefore, digestion of DNA was performed directly after nuclei isolation. This allowed proper DNA digestion and subsequent salt extraction. Subsequently, we treated the remaining nuclear fraction with RNAse to obtain solubilise candidate proteins by digesting *Xist* RNA.

In order to characterise the biochemical fractionation, we performed western blot analysis of different fractions. The nuclear scaffold factor Saf-A has been detected in the nuclear matrix fraction after chromatin removal (Helbig and Fackelmayer, 2003). Thus, Saf-A serves as a positive control for the insoluble nuclear matrix fraction. In addition, Saf-A has been reported to be enriched on the inactive X chromosome (Helbig and Fackelmayer, 2003). This localization depends on its RNA binding RGG domain, which suggests a possible direct interaction between Saf-A and Xist. Therefore, we reasoned that Saf-A might also localize in the soluble fraction after RNA digestion of the nuclear matrix in ES cells in an *Xist* dependent manner. Lamins are components of the nuclear lamina, which is a structure near the inner nuclear membrane and the peripheral chromatin. The internal lamins that connect to nuclear pore complexes are major structural elements of the internal nuclear matrix. Therefore, lamins are expected

to be in the insoluble nuclear matrix fraction. The highly abundant histones are the main protein components of chromatin, which we aimed to remove in the fractionation procedure by DNAse treatment and salt extraction.

We extracted nuclear matrix of ES 36.11 cells and performed western blot analysis of different cell fractions (Figure16). As expected, Saf-A was found to a large extent in the insoluble nuclear matrix fraction and to a minor extent in the soluble fraction after RNAse treatment. In contrast, lamines were detected only in the insoluble nuclear matrix fraction. Neither Saf-A nor lamin was observed in the cytoplasmic fraction, suggesting an isolation of intact nuclei. In the soluble fraction only a low amount of histones was detected. RNAse A, which was added in a large amount to extract the nuclear matrix fraction, did not give any background signal on Western blots revealed either with the Saf-A or lamin A antibodies.

These data indicated that, following this cell fractionation procedure, we obtained a soluble nuclear matrix fraction suitable for proteomic analysis.

The soluble fraction obtained from nuclear matrix was analysed by mass spectrometry by Karl Mechtler (Table 1). The data indicated that histone proteins are only a minor constitutent of the sample and did not prevent the identification of other less abundant nuclear proteins. Thus, our strategy of chromatin removal before candidate protein extraction was successful. We aimed at an initial comparison of samples prepared from cells treated with doxycycline for induction of *Xist* expression and untreated controls. For this we used the number of peptides identified for each protein as an indication of relative protein abundance in the samples. This is a measure which presents various caveats but can be applied for an initial characterization. A more robust approach is to measure the

peak areas of characteristic mass peaks in the spectra and set these integrated peak areas in relation. Using both methods several proteins were identified as a candidate factor that could be potentially become enriched in the nuclear matrix fraction after *Xist* expression. However, the observed enrichment was low, on average 3.5 fold and required an independent confirmation. Among the potential candidates we observed Trim28, which was of interest because it had been previously been implicated in retroviral silencing and host defense in ES cells (Wolf and Goff, 2007).

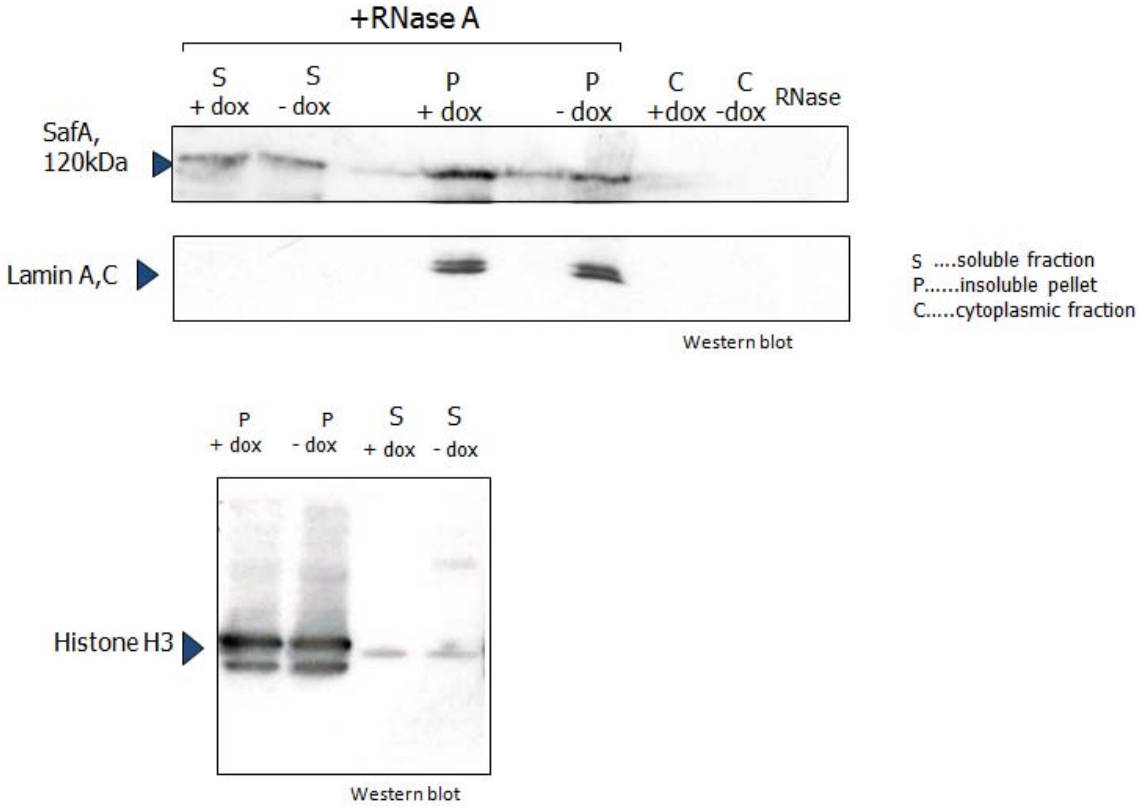


**Figure 16: Analysis of Saf-A, lamin A and histone H3 in ES 36.11 cell fractions**

ES 36.11 cells were grown for 48h followed by nuclear matrix extraction. Saf-A is shown to be abundant in the soluble as well as in the insoluble fraction, whereas lamin A was detected only in the insoluble fraction. Saf-A and Lamin A were not observed in the cytoplamsic fraction as well as in the RNAse control. Histone were only very little abundant in the soluble fraction.

The preliminary analysis of nuclear matrix extraction using glass slides showed *Xist* to remain in the matrix fraction of ES cells only after fixation. Therefore we intended to isolate the *Xist* containing fraction of fixed nuclei, using a biochemical fractionation procedure.

For this 36.11 ES cells were cultivated in the presence of doxycycline for 2 days and nuclei were isolated as described above. In order to fix nuclei, they were washed with PBS in the presence of 2mM tetrathionate sulphate for 10 minutes. Following extraction with ammonium sulphate yielded sticky nuclear pellet. We obtained nuclei, which are more stable, when we washed them with ficoll containing buffer in the presence of tetrathionate. In addition we attempted to digest DNA directly after fixation followed by salt extraction. In this way we obtained a nuclear matrix fraction that could be extracted by RNA digestion. In order to verify our fractionation procedure, we performed western blot analysis to detect Saf-A and Lamin B, which are components of the nuclear matrix (Figure 17). As expected, we identified high levels of Saf-A as well as lamin-B in the insoluble fraction of the nuclear matrix. In comparison to the fractions of unfixed nuclei, we observed that Saf-A was not solubilised after RNA digestion. This might be due to better preservation of the nuclear matrix. We observed a small amount of Saf-A in the supernatant after extraction with ammonium sulphate, meaning that a small amount of Saf-A became soluble while chromatin was soluble. Lamin B was present mainly in isolated nuclei, the supernatant after salt extraction and the insoluble nuclear matrix pellet. In contrast very little lamin B was observed in the soluble fraction after RNAse treatment. The soluble fraction after RNAse treatment of the nuclear matrix was analysed by mass spectrometry

by Karl Mechler (Table 2). Several proteins were detected in these fractions but the number of identified proteins appeared lower than of fraction from cells that were not fixed with Tetrathionate. Some proteins showed enrichment after *Xist* induction but these seemed to belong to the class of general RNA binding proteins or nucleolar components. Thus, the proteins were of little interest for followup studies as they did not provide a link to chromatin or gene regulation.

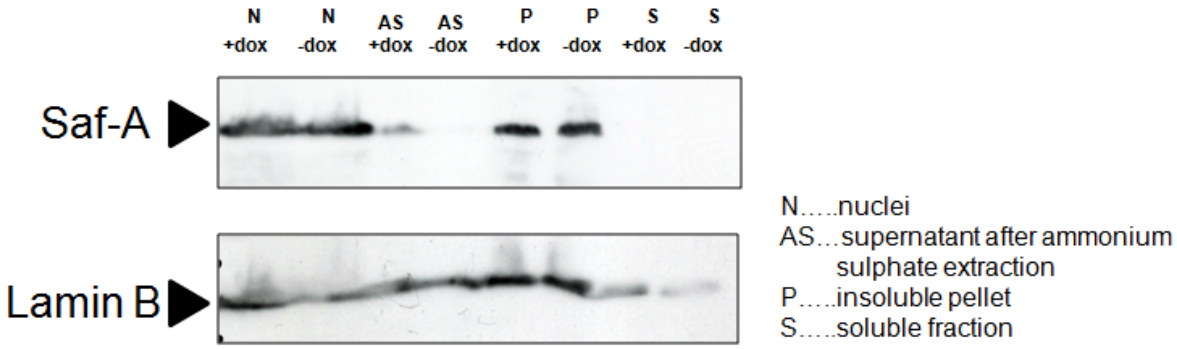


**Figure 17: Detection of Saf-A and lamin in nuclear fractions of fixed nuclei**

ES 36.11 cells were grown for 48h followed by nuclear matrix extraction. Saf-A is shown to be abundant in the insoluble fraction compared to the soluble fraction. Lamin A was detected in the insoluble fraction and showed very little lamin B was observed in the soluble fraction. Lamin A and Saf-A was detected in the nuclei.

## Analysis of Trim 28 upon *Xist* expression in ES cells

Preliminary mass spectrometric analysis of unfixed soluble fractions indicated Trim28 as a candidate factor that showed potential enrichment in the nuclear matrix fraction upon *Xist* induction. Trim 28 was of interest, because it is a known transcriptional silencer and was previously shown to repress transcription of proviral DNAs from moloney murine leukemia virus in embryonic carcinoma and ES cells (Wolf and Goff, 2007).

To confirm the abundance of Trim28 in the soluble fractions, we aimed to identify Trim28 by western blot analysis. Therefore we used an affinity purified antibody from everest biotech, which has been tested in human and mouse and recognizes a band at approximately 100 – 120kDa. Different dilutions of the antibody were tested on total ES cell extract. For this 36.11 ES cells were cultivated in the presence of doxycycline for 48 hours. For comparison, 36.11 ES cells were cultivated without *Xist* induction. Cells were harvested; total cell extract was prepared and loaded on a polyacrylamide gel. Western blot analysis showed many unspecific bands indicating antibody background staining. No band at the correct size of 100 – 120kDa was observed (data not shown). Therefore, we tried 2 further antibodies, which are commercially available: Trim28 specific antibodies from bethyl laboratories and from abcam are both affinity purified and tested in human. They identify a band at approximately 110 kDa. Different dilutions of both antibodies were tested on total ES cell extract. A strong band at the size of 120 kDa was observed using both antibodies at a high dilution (bethyl: 1:20000 and abcam: 1:2000) and thus can be regarded as

Trim28 specific. The antibody from abcam detected 2 further bands at a lower molecular weight, which are not specific for Trim28. Therefore, the best result was obtained with the antibody from bethyl at a 1:20000 dilution (data not shown).

Next, we aimed to verify the enrichment of Trim28 in the soluble fractions upon *Xist* induction, which was already shown by mass spectrometry. We performed western blot analysis using the optimized conditions and detected a band specific for Trim28 in the soluble fraction as well as in the insoluble pellet. As a control, we investigated total cell extracts, which showed a high abundance of Trim28 in ES cells. We observed that Trim28 was more abundant in the soluble fraction upon *Xist* expression (Figure 18).

Thus, we were able to confirm the results from mass spectrometric analysis, showing that Trim28 is enriched in the nuclear matrix fraction upon *Xist* induction.

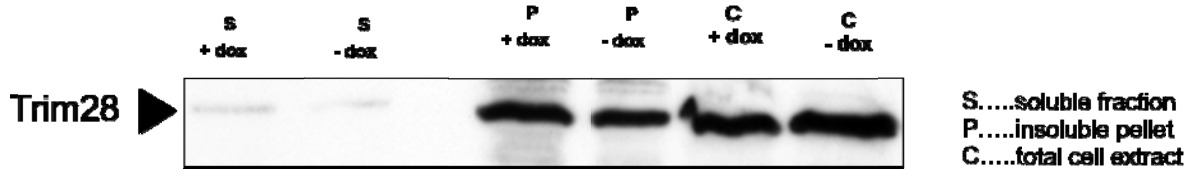


**Figure 18: Trim28 western blot analysis of unfixed ES cell fraction**

Trim28 was detected in the insoluble pellet fraction as well as total cell extract. An enrichment of Trim28 was observed in the soluble fraction upon *Xist* induction (S +dox).

Further we performed a similar analysis of Trim28 in fractions obtained after Tetrathionate fixation. Western analysis of fixed nuclear matrix extracts showed Trim28 in the insoluble pellet fraction. However, we did not observe Trim28 in the soluble fractions after RNase treatment as indicated by previous mass spectrometric analysis. A potential reason for this could be that Trim28 cannot be eluted from the matrix after fixation.

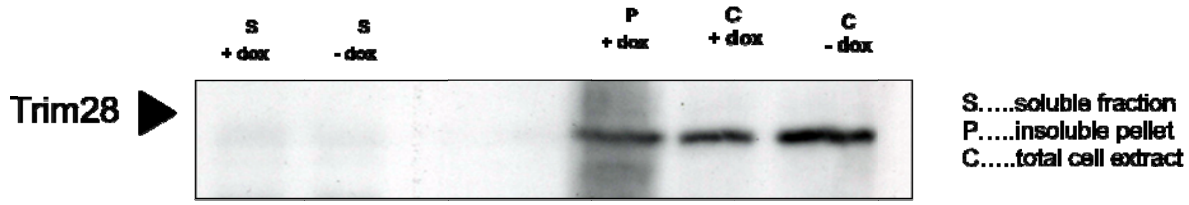


**Figure 19: Trim28 western blot of fractions from ES cell matrix preparations after sodium tetrathionate fixation**

Trim28 was detected in the insoluble pellet fractions, but not in the soluble fraction.

**Table 1: Mass spectrometric analysis of nuclear matrix extracts**
Protein name and accession number is shown for each protein. The peptide areas and their ratios are shown of canditates of intere

| Protein name | Acc. Nr. | Areas (sum of peptid-area) minus dox | plus dox | Ratio |
|---|---|---|---|---|
| Strbp :: Spermatid perinuclear RNA binding protein - Mus musculus (Mouse); Mice homozygous for a gene trap insertion exhibit premature death, a reduced body size and an abnormal clutching reflex. Minor brain abnormalities and spermatogenesis defects were also noted. | A2BH81\| | 49882607 | 193843072 | 1 : 3.89 |
| Ilf3 / NF90 :: Nuclear factor 90 - Mus musculus (Mouse) | Q45VK5\| | 146654680 | 465693087 | 1 : 3.18 |
| Ddx3x X-linked embryonic RNA helicase :: 2 cells egg cDNA, RIKEN full-length enriched library, clone:B020006B14 product:DEAD/H - Mus musculus (Mouse) | Q3TQX5 | 16552490 | 169999338 | 1 : 10.3 |
| Myef-2 :: Myelin basic protein expression factor 2, repressor - Mus musculus (Mouse) | A2ATP5\| | 8915096 | 29431584 | 1 : 3.3 |
| CRL-1722 L5178Y-R cDNA, RIKEN full-length enriched library, clone:I730096G03 product:heterogeneous nuclear ribonucleoprotein M, full insert sequence - Mus musculus (Mouse) | Q3THB3\| | | | |
| 17 days embryo heart cDNA, RIKEN full-length enriched library, clone:I920087O13 product:vimentin, full insert sequence - Mus musculus (Mouse) | Q3TFD9\| | | | |
| DEAD - Mus musculus (Mouse) | A1L333\|A | | | |
| Lung RCB-0558 LLC cDNA, RIKEN full-length enriched library, clone:G730022P12 product:heterogeneous nuclear ribonucleoprotein L, full insert sequence - Mus musculus (Mouse) | Q3UMT7 | | | |
| Dhx15 :: 16 days embryo kidney cDNA, RIKEN full-length enriched library, clone:I920087J23 product:DEAH - Mus musculus (Mouse) Dhx15 | Q3TFE5\| | 5497081 | 18413779 | 1 : 3.35 |
| Osteoclast-like cell cDNA, RIKEN full-length enriched library, clone:I420039N16 product:heterogeneous nuclear ribonucleoprotein U, full insert sequence - Mus musculus (Mouse) | Q3TVV6\| | | | |
| Mov10 :: 17 days pregnant adult female amnion cDNA, RIKEN full-length enriched library, clone:I920090G16 product:Moloney leukemia virus 10, full insert sequence - Mus musculus (Mouse) | Q3TFC0\| | 50601365 | 99000950 | 1 : 1.96 |
| 13 days embryo liver cDNA, RIKEN full-length enriched library, clone:I920036O16 product:proliferation-associated 2G4, full insert sequence - Mus musculus (Mouse) | Q3TGU7 | 13128466 | 54831764 | 1 : 4.18 |
| 2 days neonate thymus thymic cells cDNA, RIKEN full-length enriched library, clone:E430022F21 product:annexin A2, full insert sequence - Mus musculus (Mouse) | Q542G9\| | | | |
| Bone marrow macrophage cDNA, RIKEN full-length enriched library, clone:I830165N20 product:ribosomal protein S3a, full insert sequence - Mus musculus (Mouse) | Q3U5P8\| | | | |
| Insulin-like growth factor 2 mRNA binding protein 2 - Mus musculus (Mouse) | A6X8Z3\|A | nd | 41754682 | nd : 1 |
| 12 days embryo spinal ganglion cDNA, RIKEN full-length enriched library, clone:D130062P10 product:ELAV - Mus musculus (Mouse) | Q3UR02\| | 4089494 | 13659408 | 1 : 3.34 |
| Blastocyst blastocyst cDNA, RIKEN full-length enriched library, clone:I1C0040A22 product:ribosomal protein S17, full insert sequence - Mus musculus (Mouse) | Q3TK12\| | nd | 54245047 | nd : 1 |
| Heterogeneous nuclear ribonucleoprotein A3 - Mus musculus (Mouse) | A2AL12\|A | | | |
| matrin 3 :: 10 days neonate skin cDNA, RIKEN full-length enriched library, clone:4732457K09 product:matrin 3, full insert sequence - Mus musculus (Mouse) | Q3TTX0\| | 80669494 | 323605916 | 1 : 4.01 |
| S1 protein C2 - Mus musculus (Mouse) | Q20BD0\| | | | |
| Non-muscle alpha-actinin 4 - Mus musculus (Mouse) | Q1A602\| | | | |
| Ribosomal protein S3 - Mus musculus (Mouse) | Q5YLW3 | | | |
| Rps9 protein - Mus musculus (Mouse) | Q96EC0\| | | | |
| 2 days neonate thymus thymic cells cDNA, RIKEN full-length enriched library, clone:E430001E01 product:ribosomal protein L10A, full insert sequence - Mus musculus (Mouse) | Q3U561\| | | | |
| U1 small nuclear ribonucleoprotein polypeptide A - Mus musculus (Mouse) | A2RS68\| | | | |
| Bone marrow macrophage cDNA, RIKEN full-length enriched library, clone:I830128K02 product:RNA binding motif protein 14, full insert sequence - Mus musculus (Mouse) | Q3U6A2\| | | | |
| MCM3 :: 17 days embryo heart cDNA, RIKEN full-length enriched library, clone:I920096F09 product:DNA replication licensing factor MCM3 - Mus musculus (Mouse) | Q3UI57\|C | nd | 10832015 | nd : 1 |
| Rbm39 protein - Mus musculus (Mouse) | Q0VGU9 | | | |
| Rpl30 protein - Mus musculus (Mouse) | Q497D7\| | | | |
| Ribosomal protein S25 - Mus musculus (Mouse) | Q58EA6\| | | | |
| Rpl17 protein - Mus musculus (Mouse) | Q505B1\| | | | |
| Ras-GTPase-activating protein binding protein 2 - Mus musculus (Mouse) :: 2 days neonate thymus thymic cells cDNA, RIKEN full-length enriched library, clone:E430003G24 product:Ras-GTPase-activating protein binding protein 2 - Mus musculus (Mouse) | Q3U541\| | nd | 17408498 | nd : 1 |
| importin alpha :: Karyopherin - Mus musculus (Mouse) | Q52L97\|C | nd | 14968214 | nd : 1 |
| 12 days embryo spinal ganglion cDNA, RIKEN full-length enriched library, clone:D130013C23 product:DEAH - Mus musculus (Mouse) | Q3UR42\| | | | |
| Actin, gamma, cytoplasmic 1 - Mus musculus (Mouse) | Q4KL81\| | | | |

| | | | | |
|---|---|---|---|---|
| Bone marrow macrophage cDNA, RIKEN full-length enriched library, clone:I830015L07 product:nuclease sensitive element binding protein 1, full insert sequence - Mus musculus (Mouse) | Q3UBT1\| | | | |
| ELAV-LIKE PROTEIN 1 :: 12 days embryo embryonic body between diaphragm region and neck cDNA, RIKEN full-length enriched library, clone:9430002B02 product:ELAV-LIKE PROTEIN 1 - Mus musculus (Mouse) | Q8BM84 | 170127674 | 469842908 | 1 : 2.76 |
| Poly A binding protein, cytoplasmic 4 - Mus musculus (Mouse) | A3KFU5\| | | | |
| TRIM28 :: Tripartite motif protein 28 - Mus musculus (Mouse) | Q5EBP9\| | 19472290 | 64635464 | 1 : 3.32 |
| Bone marrow macrophage cDNA, RIKEN full-length enriched library, clone:I830035O17 product:**ribosomal protein L3**, full insert sequence - Mus musculus (Mouse) | Q3U9L3\| | 14353175 | 40426566 | 1 : 2.82 |
| 2 days neonate thymus thymic cells cDNA, RIKEN full-length enriched library, clone:E430010B17 product:ribosomal protein L4, cytosolic homolog - Mus musculus (Mouse) | Q564E8\| | | | |
| Adult male testis cDNA, RIKEN full-length enriched library, clone:1700012H05 product:TESTES SPECIFIC HETEROGENOUS NUCLEAR RIBONUCLEOPROTEIN G-T homolog - Mus musculus (Mouse) | Q9DAE2 | | | |
| 3 days neonate thymus cDNA, RIKEN full-length enriched library, clone:A630098I22 product:TAR DNA binding protein, full insert sequence - Mus musculus (Mouse) | Q3U591\| | | | |
| Rpl23a protein - Mus musculus (Mouse) | Q4V9X9\| | | | |
| Osteoclast-like cell cDNA, RIKEN full-length enriched library, clone:I420032B10 product:ribosomal protein S18, full insert sequence - Mus musculus (Mouse) | Q3TW65 | | | |
| Ribosomal protein S8 - Mus musculus (Mouse) | Q497E9\| | | | |
| CRL-1722 L5178Y-R cDNA, RIKEN full-length enriched library, clone:I730084D22 product:Hypothetical RNA binding protein RDA288 homolog - Mus musculus (Mouse) | Q3UJK2\| | | | |
| 60S acidic ribosomal protein P0 - Mus musculus (Mouse) | Q5FWB6 | | | |
| Activated spleen cDNA, RIKEN full-length enriched library, clone:F830208A11 product:DEAD - Mus musculus (Mouse) | Q3T9L0\| | | | |
| Ribosomal protein L7a - Mus musculus (Mouse) | Q58ET1\| | | | |
| Bone marrow macrophage cDNA, RIKEN full-length enriched library, clone:I830082P18 product:ribosomal protein L15, full insert sequence - Mus musculus (Mouse) | Q3U7D2\| | | | |
| ***15 days pregnant adult female placenta cDNA, RIKEN full-length enriched library, clone:I530023K22 product:tropomyosin 3, gamma, full insert sequence - Mus musculus (Mouse)*** | ***Q3TJ53\|*** | | | |
| 60S ribosomal protein L6 - Mus musculus (Mouse) | Q3UCH0 | | | |
| Small nuclear ribonucleoprotein D3 - Mus musculus (Mouse) | Q91VM2 | | | |
| ***Hnrpf protein - Mus musculus (Mouse) hnRNP F*** | ***Q8R582\|*** | | | |
| Heterogeneous nuclear ribonucleoprotein H2 - Mus musculus (Mouse) | A2BDV8\| | | | |
| Sf3b1 protein - Mus musculus (Mouse) | A0JLN0\| | 783400 | 1064688 | 1 : 1.36 |
| CRL-1722 L5178Y-R cDNA, RIKEN full-length enriched library, clone:I730098H14 product:splicing factor, arginine/serine-rich 7, full insert sequence - Mus musculus (Mouse) | Q3THA6\| | | | |
| Splicing factor proline/glutamine rich - Mus musculus (Mouse) | A2A7U6\| | | | |
| Ribosomal protein L14 - Mus musculus (Mouse) | Q569Z0\| | | | |
| 60S ribosomal protein L36 - Mus musculus (Mouse) | Q5M9L1\| | | | |
| OTTMUSP00000017203 - Mus musculus (Mouse) | A3KGK6\| | | | |
| ***Zfp326 Zn-finger nucl. Matrix 16 :: days neonate thymus cDNA, RIKEN full-length enriched library, clone:A130002H22 product:zinc finger protein 326, full insert sequence. - Mus musculus (Mouse)*** | ***Q3TRI9\|*** | | | |
| Sf3b2 :: Bone marrow macrophage cDNA, RIKEN full-length enriched library, clone:I830028H02 product:splicing factor 3b, subunit 2, full insert sequence - Mus musculus (Mouse) | Q3UAI4\| | nd | 24338481 | nd : 1 |
| Annexin A11 - Mus musculus (Mouse) | Q921F1\| | | | |
| Far upstream element - Mus musculus (Mouse) FuBp3 | A2AJ72\| | nd | 22006945 | nd : 1 |
| Ribosomal protein L19 - Mus musculus (Mouse) | A2A547\| | | | |
| Rps19 protein - Mus musculus (Mouse) | Q5M9P3 | | | |
| Mi2beta = Chd4 -> NuRD :: MKIAA4075 protein - Mus musculus (Mouse) | Q5DTP7\| | nd | 13129123 | nd : 1 |
| nucleolin :: Blastocyst blastocyst cDNA, RIKEN full-length enriched library, clone:I1C0002A07 product:nucleolin, full insert sequence - Mus musculus (Mouse) | Q3TL52\| | 1,522E+09 | 4833901496 | 1 :3.18 |
| Bone marrow macrophage cDNA, RIKEN full-length enriched library, clone:I830045N07 product:heterogeneous nuclear ribonucleoprotein R, full insert sequence - Mus musculus (Mouse) | Q3U8W9 | | | |
| Ilf2 :: 12 days embryo female mullerian duct includes surrounding region cDNA, RIKEN full-length enriched library, clone:6820446H05 product:interleukin enhancer binding factor 2, full insert sequence - Mus musculus (Mouse) | Q3UXI9\| | 107790080 | 660508460 | 1 : 6.13 |
| Heterogeneous nuclear ribonucleoprotein H1 - Mus musculus (Mouse) | Q811L7\| | | | |
| In vitro fertilized eggs cDNA, RIKEN full-length enriched library, clone:7420408C23 product:heterogeneous nuclear ribonucleoprotein D, full insert sequence. - Mus musculus (Mouse) | Q3UXC8 | | | |
| Elongation factor 1-alpha - Mus musculus (Mouse) | Q3TII3\|Q | 11841542 | 66563102 | 1 : 5.62 |
| TIB-55 BB88 cDNA, RIKEN full-length enriched library, clone:I730008D20 product:ribosomal protein L12, full insert sequence - Mus musculus (Mouse) | Q3TIQ2\| | | | |

| | | | | |
|---|---|---|---|---|
| 12 days embryo embryonic body between diaphragm region and neck cDNA, RIKEN full-length enriched library, clone:9430049D01 product:synaptotagmin binding, cytoplasmic RNA interacting protein, full insert seque... - Mus musculus (Mouse) | Q3TRV3\| | | | |
| MKIAA0138 protein - Mus musculus (Mouse) | Q6A0C0\| | | | |
| Ribosomal protein S21 - Mus musculus (Mouse) | A2ABW8 | | | |
| Nuclear pore complex-associated intranuclear coiled-coil protein TPR - Mus musculus (Mouse) | Q7M739\| | | | |
| CRL-1722 L5178Y-R cDNA, RIKEN full-length enriched library, clone:I730073G06 product:60S ribosomal protein L18a, full insert sequence - Mus musculus (Mouse) | Q3THJ0\| | | | |
| 1 cell embryo 1 cell cDNA, RIKEN full-length enriched library, clone:I0C0016F01 product:TAF15 RNA polymerase II, TATA box binding protein - Mus musculus (Mouse) | Q3TLE4\| | | | |
| CRL-1722 L5178Y-R cDNA, RIKEN full-length enriched library, clone:I730022O16 product:ribosomal protein S15, full insert sequence - Mus musculus (Mouse) | Q3UK70\| | | | |
| Alpha actinin 1a - Mus musculus (Mouse) | A1BN54\| | | | |
| 17 days embryo kidney cDNA, RIKEN full-length enriched library, clone:I920078L09 product:FUS interacting protein - Mus musculus (Mouse) | Q3TFP0\| | | | |
| Mcm5 :: Minichromosome maintenance deficient 5, cell division cycle 46 - Mus musculus (Mouse) | Q52KC3\| | 1103857 | 6564275 | 1 : 5.95 |
| 12 days embryo male wolffian duct includes surrounding region cDNA, RIKEN full-length enriched library, clone:6720473C09 product:small nuclear ribonucleoprotein polypeptide A', full insert sequence - Mus musculus (Mouse) | Q8BSH5 | | | |
| NOD-derived CD11c +ve dendritic cells cDNA, RIKEN full-length enriched library, clone:F630010M18 product:ribosomal protein L13a, full insert sequence - Mus musculus (Mouse) | Q3TDS9\| | | | |
| Ribosomal protein L28 - Mus musculus (Mouse) | Q5M9J8\| | | | |
| Ribosomal protein L38 - Mus musculus (Mouse) | Q52KP0\| | | | |
| Ribosomal protein S15a - Mus musculus (Mouse) | Q5M9M4 | | | |
| Ribosomal protein L11 - Mus musculus (Mouse) | A2BH06\| | | | |
| Ahnak protein - Mus musculus (Mouse) | A0JLR7\|A | | | |
| Puf60 protein - Mus musculus (Mouse) FIR | Q0VDY2 | nd | 12346746 | nd : 1 |
| Peptidyl-prolyl cis-trans isomerase - Mus musculus (Mouse) | Q3UBU9 | | | |
| Rpl18 protein - Mus musculus (Mouse) | Q58EW0 | | | |
| Grwd1 protein - Mus musculus (Mouse) | Q5XJZ3\| | | | |
| Processing of 1, ribonuclease P/MRP family, - Mus musculus (Mouse) | Q8K205\| | | | |
| 0 day neonate thymus cDNA, RIKEN full-length enriched library, clone:A430101M19 product:ribosomal protein S5, full insert sequence - Mus musculus (Mouse) | Q91V55\| | | | |
| 10, 11 days embryo whole body cDNA, RIKEN full-length enriched library, clone:2810036L13 product:SIMILAR TO SMOOTH homolog - Mus musculus (Mouse) | Q9CSH0 | | | |
| Splicing factor 3a, subunit 3 - Mus musculus (Mouse) | Q58E59\| | nd | 11120634 | nd : 1 |
| Ribosomal protein L9 - Mus musculus (Mouse) | Q5EBQ6 | | | |
| Sf3a1 :: Osteoclast-like cell cDNA, RIKEN full-length enriched library, clone:I420047E18 product:splicing factor 3a, subunit 1, full insert sequence - Mus musculus (Mouse) | Q3TVM1 | nd | 6365837 | nd : 1 |
| Tyrosine 3-monooxygenase/tryptophan 5-monooxygenase activation protein, epsilon polypeptide - Mus musculus (Mouse) | Q5SS40\| | | | |
| 6 days neonate spleen cDNA, RIKEN full-length enriched library, clone:F430009E14 product:thymopoietin, full insert sequence - Mus musculus (Mouse) | Q3TNH0 | | | |
| clone:I830046M23 product:poly A binding protein, cytoplasmic 1, full insert sequence - | Q3U8U8\| | | | |
| 5 days embryo whole body cDNA, RIKEN full-length enriched library, clone:I0C0047C10 product:heterogeneous nuclear ribonucleoprotein K, full insert sequence - Mus musculus (Mouse) | Q3TL71\| | | | |
| 17 days pregnant adult female amnion cDNA, RIKEN full-length enriched library, clone:I920058I09 product:Sjogren syndrome antigen B, full insert sequence - Mus musculus (Mouse) | Q3TG93\| | | | |
| B6-derived CD11 +ve dendritic cells cDNA, RIKEN full-length enriched library, clone:F730215J21 product:heat shock protein 8, full insert sequence. - Mus musculus (Mouse) | Q3TB63\| | | | |
| MRT4, mRNA turnover 4, homolog - Mus musculus (Mouse) | A2AMU9 | | | |
| CRL-1722 L5178Y-R cDNA, RIKEN full-length enriched library, clone:I730064N19 product:guanine nucleotide binding protein, beta 2, related sequence 1, full insert sequence - Mus musculus (Mouse) | Q3THP0\| | | | |
| D19Bwg1357e protein - Mus musculus (Mouse) | Q7TMX0 | | | |
| Tcof1 protein - Mus musculus (Mouse) | Q05BH6\| | | | |
| CDNA, RIKEN full-length enriched library, clone:I920161F21 product:poly(rC) binding protein 2, full insert sequence - Mus musculus (Mouse) | Q3TF69\| | | | |
| 12 days embryo female mullerian duct includes surrounding region cDNA, RIKEN full-length enriched library, clone:6820407G10 product:ribosomal protein S4, X-linked, full insert sequence - Mus musculus (Mouse) | Q3UXQ6 | | | |

| | | | | |
|---|---|---|---|---|
| B16 F10Y cells cDNA, RIKEN full-length enriched library, clone:G370049E15 product:GPI-anchored membrane protein 1, full insert sequence. - Mus musculus (Mouse) | Q3UFZ6\| | | | |
| 16 days embryo head cDNA, RIKEN full-length enriched library, clone:C130041B04 product:annexin A1, full insert sequence - Mus musculus (Mouse) | Q3US43\| | | | |
| Blastocyst blastocyst cDNA, RIKEN full-length enriched library, clone:I1C0037A13 product:hypothetical Zn-finger, C-x8-C-x5-C-x3-H type containing protein, full insert sequence - Mus musculus (Mouse) | Q3UL31\| | | | |
| Rps16 protein - Mus musculus (Mouse) | A4FUS1\| | | | |
| 40S ribosomal protein S12 - Mus musculus (Mouse) | Q6ZWZ6 | | | |
| 60S ribosomal protein L27 - Mus musculus (Mouse) | Q5BLJ9\| | | | |
| Small nuclear ribonucleoprotein B - Mus musculus (Mouse) | A2APD4\| | | | |
| Ribosomal protein L37a - Mus musculus (Mouse) | Q4VAF2\| | | | |
| Ribosomal protein L22 - Mus musculus (Mouse) | Q4VAG4 | | | |
| ES cells cDNA, RIKEN full-length enriched library, clone:2400004P05 product:ribosomal protein L27a, full insert sequence - Mus musculus (Mouse) | Q9CQ16 | | | |
| Peptidyl-prolyl cis-trans isomerase - Mus musculus (Mouse) | Q9DCY1 | | | |
| Bone marrow macrophage cDNA, RIKEN full-length enriched library, clone:I830014L05 product:ribosomal protein S11, full insert sequence - Mus musculus (Mouse) | Q3UC02\| | | | |
| TIB-55 BB88 cDNA, RIKEN full-length enriched library, clone:I730044G20 product:ribosomal protein S2, full insert sequence - Mus musculus (Mouse) | Q3TI78\|Q | | | |
| RNP particle component - Mus musculus (Mouse) | O08905\|Q | | | |
| MKIAA4115 protein - Mus musculus (Mouse) | Q571F9\|Q | | | |
| Anxa6 protein - Mus musculus (Mouse) | Q99JX6\|Q | | | |
| CRL-1722 L5178Y-R cDNA, RIKEN full-length enriched library, clone:I730029B08 product:heterogeneous nuclear ribonucleoprotein A1, full insert sequence - Mus musculus (Mouse) | Q3TIK8\|Q | | | |
| Bone marrow macrophage cDNA, RIKEN full-length enriched library, clone:I830120C02 product:heterogeneous nuclear ribonucleoprotein C, full insert sequence - Mus musculus (Mouse) | Q3U6P5\| | | | |
| HnRNP-associated with lethal yellow - Mus musculus (Mouse) | A2AU62\| | | | |
| Rbmxrt protein - Mus musculus (Mouse) | Q91VM5 | | | |
| TIB-55 BB88 cDNA, RIKEN full-length enriched library, clone:I730032G19 product:RNA-binding protein FUS - Mus musculus (Mouse) | Q3UK30\| | | | |
| Histone H4 - Mus musculus (Mouse) | A0AUM5 | 50137141 | 174603342 | 1 : 3.48 |
| 17 days embryo kidney cDNA, RIKEN full-length enriched library, clone:I920097C16 product:DEAH - Mus musculus (Mouse) | Q3TF92\|Q | | | |
| TIB-55 BB88 cDNA, RIKEN full-length enriched library, clone:I730090E06 product:ribosomal protein L5, full insert sequence. - Mus musculus (Mouse) | Q3THE1\| | | | |
| Chromobox homolog 3 - Mus musculus (Mouse) | Q32P00\|Q | | | |
| 2 days neonate thymus thymic cells cDNA, RIKEN full-length enriched library, clone:E430001A02 product:high mobility group box 2, full insert sequence - Mus musculus (Mouse) | Q3U566\| | | | |
| NOD-derived CD11c +ve dendritic cells cDNA, RIKEN full-length enriched library, clone:F630119J17 product:MYB binding protein - Mus musculus (Mouse) | Q3U2W2 | | | |
| Npm1 protein - Mus musculus (Mouse) | Q5BL09\|Q | 4872664 | 6942082 | 1 : 1.43 |
| Activated spleen cDNA, RIKEN full-length enriched library, clone:F830304D19 product:polypyrimidine tract binding protein 1, full insert sequence - Mus musculus (Mouse) | Q3T984\|Q | | | |
| Bone marrow macrophage cDNA, RIKEN full-length enriched library, clone:I830018I23 product:ribosomal protein L7, full insert sequence - Mus musculus (Mouse) | Q3UBI6\|Q | | | |
| 10 day old male pancreas cDNA, RIKEN full-length enriched library, clone:1810006O06 product:RNA binding motif protein 3, full insert sequence - Mus musculus (Mouse) | Q545K5\|Q | | | |
| Bone marrow macrophage cDNA, RIKEN full-length enriched library, clone:I830085L15 product:splicing factor, arginine/serine-rich 3 - Mus musculus (Mouse) | Q3U781\| | | | |
| Zfp326 protein - Mus musculus (Mouse) | Q05DP5\| | | | |
| Bone marrow macrophage cDNA, RIKEN full-length enriched library, clone:I830080I04 product:ribosomal protein L26, full insert sequence - Mus musculus (Mouse) | Q3U7N1\| | | | |
| 10 days neonate cerebellum cDNA, RIKEN full-length enriched library, clone:6530441M19 product:U6 SNRNA-ASSOCIATED SM-LIKE PROTEIN LSM6 homolog - Mus musculus (Mouse) | Q542U7\| | | | |
| TIB-55 BB88 cDNA, RIKEN full-length enriched library, clone:I730091D16 product:ribosomal protein L8, full insert sequence - Mus musculus (Mouse) | Q3THC7 | | | |
| Eukaryotic translation elongation factor 1 delta - Mus musculus (Mouse) | Q68FG5\| | | | |
| Novel protein silmilar to ribosomal protein L32 - Mus musculus (Mouse) | A2AD25\| | | | |
| Rps28 protein - Mus musculus (Mouse) | Q059I1\|Q | | | |
| Bone marrow macrophage cDNA, RIKEN full-length enriched library, clone:I830030H04 product:H2A histone family, member Z, full insert sequence - Mus musculus (Mouse) | Q3UA95\| | | | |
| Ribosomal protein S23 - Mus musculus (Mouse) | Q497E1\|Q | | | |

| | | | | |
|---|---|---|---|---|
| 12 days embryo head cDNA, RIKEN full-length enriched library, clone:3010002H06 product:small nuclear ribonucleoprotein polypeptide A, full insert sequence - Mus musculus (Mouse) | Q9CXX7 | | | |
| 60S ribosomal protein L13 - Mus musculus (Mouse) | Q5RKP3 | | | |
| Adult male epididymis cDNA, RIKEN full-length enriched library, clone:9230011J09 product:ribosomal protein L24, full insert sequence - Mus musculus (Mouse) | Q3UW40 | | | |
| CRL-1722 L5178Y-R cDNA, RIKEN full-length enriched library, clone:I730071I06 product:ribosomal protein 10, full insert sequence - Mus musculus (Mouse) | Q3THJ6\| | | | |
| Osteoclast-like cell cDNA, RIKEN full-length enriched library, clone:I420048M08 product:DEAD - Mus musculus (Mouse) | Q3TVJ3\| | | | |
| Small nuclear ribonucleoprotein D2 - Mus musculus (Mouse) | Q14AF6\| | | | |
| CRL-1722 L5178Y-R cDNA, RIKEN full-length enriched library, clone:I730023C04 product:nascent polypeptide-associated complex alpha polypeptide, full insert sequence - Mus musculus (Mouse) | Q3UK68\| | | | |
| Eukaryotic translation elongation factor 1 gamma - Mus musculus (Mouse) | Q4FZK2\| | | | |
| 12 days embryo head cDNA, RIKEN full-length enriched library, clone:3010025E17 product:Heterogeneous nuclear ribonucleoprotein A0 - Mus musculus (Mouse) | Q9CX86\| | | | |
| Ribosomal protein S13 - Mus musculus (Mouse) | Q5BLJ7\| | | | |
| Ribosomal protein S6 - Mus musculus (Mouse) | Q5BLK1\| | | | |
| Histone H2B - Mus musculus (Mouse) | A0JLV3\| | 40678518 | 78337773 | 1 : 1.93 |
| Ribosomal protein L21 - Mus musculus (Mouse) | Q4VA28\| | | | |
| Csda protein - Mus musculus (Mouse) | Q68G78\| | | | |
| SET translocation - Mus musculus (Mouse) | A2BE93\| | | | |
| Cytochrome c, testis - Mus musculus (Mouse) | A2ARH7\| | | | |
| Chromobox homolog 1 - Mus musculus (Mouse) | A2A6C8\| | | | |
| SMT3 suppressor of mif two 3 homolog 2 - Mus musculus (Mouse) | A2A9X2\| | | | |
| Retinoblastoma binding protein 4 - Mus musculus (Mouse) | A2A875\| | | | |
| RNA binding motif protein 17 - Mus musculus (Mouse) | A2AP41\| | | | |
| KH domain containing, RNA binding, signal transduction associated 1 - Mus musculus (Mouse) | A2ACH3\| | | | |
| 13 days embryo liver cDNA, RIKEN full-length enriched library, clone:2510005B08 product:U6 snRNA-associated SM-like protein 4, full insert sequence - Mus musculus (Mouse) | Q9CY46\| | | | |
| Muscle protein 684 - Mus musculus (Mouse) | Q9QYY3 | | | |
| Osteoclast-like cell cDNA, RIKEN full-length enriched library, clone:I420007N06 product:splicing factor, arginine/serine rich 9, full insert sequence - Mus musculus (Mouse) | Q3TXM9 | | | |
| PBK1 - Mus musculus domesticus (western European house mouse) | Q1PG84\| | | | |
| Copine III - Mus musculus (Mouse) | A2AGJ0\| | | | |
| 17 days embryo heart cDNA, RIKEN full-length enriched library, clone:I920072D16 product:actin, alpha, cardiac, full insert sequence - Mus musculus (Mouse) | Q3UIJ3\| | | | |

**Table 2: Mass spectrometric analysis of nulcear matrix fractions after sodium tetrathionate fixation**
The number of peptide hits, accession number and the protein name is given of each protein.

| Protein name | Acc. Nr. | noDox | Dox | DIF |
|---|---|---|---|---|
| Bone marrow macrophage cDNA, RIKEN full-length enriched library, clone:G530123O18 product:actinin alpha 4, full insert sequence - Mus musculus (Mouse) | Q3UDJ7\|Q | 8 | 18 | 10 |
| Alpha actinin 1a - Mus musculus (Mouse) | A1BN54\|A | 0 | 10 | 10 |
| Nuclear factor 90 - Mus musculus (Mouse) | Q45VK5\|Q | 5 | 12 | 7 |
| nucleolin :: Blastocyst blastocyst cDNA, RIKEN full-length enriched library, clone:I1C0002A07 product:nucleolin, full insert sequence - Mus musculus (Mouse) | Q3TL52\|Q | 34 | 40 | 6 |
| Bone marrow macrophage cDNA, RIKEN full-length enriched library, clone:I830119C09 product:vimentin, full insert sequence - Mus musculus (Mouse) | Q3U6S1\|Q | 8 | 14 | 6 |
| 5 days embryo whole body cDNA, RIKEN full-length enriched library, clone:I0C0047C10 product:heterogeneous nuclear ribonucleoprotein K, full insert sequence - Mus musculus (Mouse) | Q3TL71\|Q | 5 | 11 | 6 |
| importin a2 :: Karyopherin - Mus musculus (Mouse) | Q52L97\|Q | 0 | 6 | 6 |
| YB-1 :: Bone marrow macrophage cDNA, RIKEN full-length enriched library, clone:I830015L07 product:nuclease sensitive element binding protein 1, full insert sequence - Mus musculus (Mouse) | Q3UBT1\|Q | 3 | 8 | 5 |
| Bone marrow macrophage cDNA, RIKEN full-length enriched library, clone:I830082P18 product:ribosomal protein L15, full insert sequence - Mus musculus (Mouse) | Q3U7D2\|Q | 0 | 5 | 5 |
| Heterogeneous nuclear ribonucleoprotein A3 - Mus musculus (Mouse) | A2AL12\|A2 | 0 | 5 | 5 |
| Rpl17 protein - Mus musculus (Mouse) | Q505B1\|Q | 0 | 5 | 5 |
| CRL-1722 L5178Y-R cDNA, RIKEN full-length enriched library, clone:I730029B08 product:heterogeneous nuclear ribonucleoprotein A1, full insert sequence - Mus musculus (Mouse) | Q3TIK8\|Q3 | 11 | 15 | 4 |
| SAF-A :: Osteoclast-like cell cDNA, RIKEN full-length enriched library, clone:I420039N16 product:heterogeneous nuclear ribonucleoprotein U, full insert sequence - Mus musculus (Mouse) | Q3TVV6\|Q | 3 | 7 | 4 |
| Histone H2B - Mus musculus (Mouse) | A0JLV3\|A0 | 2 | 6 | 4 |
| Ilf2 :: 12 days embryo female mullerian duct includes surrounding region cDNA, RIKEN full-length enriched library, clone:6820446H05 product:interleukin enhancer binding factor 2, full insert sequence - Mus musculus (Mouse) | Q3UXI9\|Q | 2 | 6 | 4 |
| Bone marrow macrophage cDNA, RIKEN full-length enriched library, clone:I830165N20 product:ribosomal protein S3a, full insert sequence - Mus musculus (Mouse) | Q3U5P8\|Q | 2 | 6 | 4 |
| 12 days embryo female mullerian duct includes surrounding region cDNA, RIKEN full-length enriched library, clone:6820407G10 product:ribosomal protein S4, X-linked, full insert sequence - Mus musculus (Mouse) | Q3UXQ6\|Q | 0 | 4 | 4 |
| Rps16 protein - Mus musculus (Mouse) | A4FUS1\|A | 0 | 4 | 4 |
| importin a2 :: 17 days embryo stomach cDNA, RIKEN full-length enriched library, clone:I920087J04 product:karyopherin - Mus musculus (Mouse) | Q3TFE8\|Q | 0 | 4 | 4 |
| Hsp90aa1 protein - Mus musculus (Mouse) | A0PJ91\|A0 | 0 | 4 | 4 |
| TIB-55 BB88 cDNA, RIKEN full-length enriched library, clone:I730090E06 product:ribosomal protein L5, full insert sequence - Mus musculus (Mouse) | Q3THE1\|Q | 0 | 4 | 4 |
| HuR; ELAV :: Adult pancreas islet cells cDNA, RIKEN full-length enriched library, clone:C820018E11 product:ELAV - Mus musculus (Mouse) | Q3UFF9\|Q | 0 | 4 | 4 |
| Bone marrow macrophage cDNA, RIKEN full-length enriched library, clone:I830046M23 product:poly A binding protein, cytoplasmic 1, full insert sequence - Mus musculus (Mouse) | Q3U8U8\|Q | 19 | 22 | 3 |
| Elongation factor 1-alpha - Mus musculus (Mouse) | Q3TII3\|Q3 | 7 | 10 | 3 |
| Bone marrow macrophage cDNA, RIKEN full-length enriched library, clone:I830120C02 product:heterogeneous nuclear ribonucleoprotein C, full insert sequence - Mus musculus (Mouse) | Q3U6P5\|Q | 6 | 9 | 3 |
| Activated spleen cDNA, RIKEN full-length enriched library, clone:F830304D19 product:polypyrimidine tract binding protein 1, full insert sequence - Mus musculus (Mouse) | Q3T984\|Q | 3 | 6 | 3 |
| Heterogeneous nuclear ribonucleoprotein H1 - Mus musculus (Mouse) | Q811L7\|Q | 2 | 5 | 3 |
| ras associated endonuclease G3Bp :: MKIAA4115 protein - Mus musculus (Mouse) | Q571F9\|Q | 0 | 3 | 3 |
| La :: 17 days pregnant adult female amnion cDNA, RIKEN full-length enriched library, clone:I920058I09 product:Sjogren syndrome antigen B, full insert sequence - Mus musculus (Mouse) | Q3TG93\|Q | 0 | 3 | 3 |
| CRL-1722 L5178Y-R cDNA, RIKEN full-length enriched library, clone:I730023C04 product:nascent polypeptide-associated complex alpha polypeptide, full insert sequence - Mus musculus (Mouse) | Q3UK68\|Q | 0 | 3 | 3 |
| Osteoclast-like cell cDNA, RIKEN full-length enriched library, clone:I420032B10 product:ribosomal protein S18, full insert sequence - Mus musculus (Mouse) | Q3TW65\|Q | 0 | 3 | 3 |
| In vitro fertilized eggs cDNA, RIKEN full-length enriched library, clone:7420408C23 product:heterogeneous nuclear ribonucleoprotein D, full insert sequence - Mus musculus (Mouse) | Q3UXC8\|Q | 0 | 3 | 3 |
| PCNA :: 2 days neonate thymus thymic cells cDNA, RIKEN full-length enriched library, clone:E430008I01 product:proliferating cell nuclear antigen, full insert sequence - Mus musculus (Mouse) | Q542J9\|Q5 | 0 | 3 | 3 |

| | | | | |
|---|---|---|---|---|
| Bone marrow macrophage cDNA, RIKEN full-length enriched library, clone:I830045N07 product:heterogeneous nuclear ribonucleoprotein R, full insert sequence - Mus musculus (Mouse) | Q3U8W9\|( | 0 | 3 | 3 |
| Ribosomal protein S14 - Mus musculus (Mouse) | O70569\|O | 0 | 3 | 3 |
| Eukaryotic translation elongation factor 1 gamma - Mus musculus (Mouse) | Q4FZK2\|Q | 0 | 3 | 3 |
| Histone cluster 1, H1d - Mus musculus (Mouse) | Q149Z9\|Q | 0 | 3 | 3 |
| Tarbp :: 3 days neonate thymus cDNA, RIKEN full-length enriched library, clone:A630098I22 product:TAR DNA binding protein, full insert sequence - Mus musculus (Mouse) | Q3U591\|Q | 0 | 3 | 3 |
| Histone H3 - Mus musculus (Mouse) | A1L0U3\|A | 0 | 3 | 3 |
| Tpr/Mlp1/Mlp2/megator :: Nuclear pore complex-associated intranuclear coiled-coil protein TPR - Mus musculus (Mouse) | Q7M739\|Q | 11 | 13 | 2 |
| S1 protein C2 - Mus musculus (Mouse) | Q20BD0\|Q | 8 | 10 | 2 |
| 14-3-3 :: Tyrosine 3-monooxygenase/tryptophan 5-monooxygenase activation protein, epsilon polypeptide - Mus musculus (Mouse) | Q5SS40\|Q | 5 | 7 | 2 |
| 60S acidic ribosomal protein P0 - Mus musculus (Mouse) | Q5FWB6\|( | 4 | 6 | 2 |
| Peptidyl-prolyl cis-trans isomerase - Mus musculus (Mouse) | Q3TE63\|Q | 3 | 5 | 2 |
| LOC665931 protein - Mus musculus (Mouse) | Q7TNQ6\|( | 3 | 5 | 2 |
| Histone H2A - Mus musculus (Mouse) | A0AUV1\|A | 2 | 4 | 2 |
| Ribosomal protein S13 - Mus musculus (Mouse) | Q5BLJ7\|Q | 0 | 2 | 2 |
| Ribosomal protein L9 - Mus musculus (Mouse) | Q5EBQ6\|( | 0 | 2 | 2 |
| Ribosomal protein L19 - Mus musculus (Mouse) | A2A547\|A: | 0 | 2 | 2 |
| Ribosomal protein S21 - Mus musculus (Mouse) | A2ABW8\|A | 0 | 2 | 2 |
| 2 days neonate thymus thymic cells cDNA, RIKEN full-length enriched library, clone:E430001E01 product:ribosomal protein L10A, full insert sequence - Mus musculus (Mouse) | Q3U561\|Q | 0 | 2 | 2 |
| CRL-1722 L5178Y-R cDNA, RIKEN full-length enriched library, clone:I730056L04 product:ribosomal protein L8, full insert sequence - Mus musculus (Mouse) | Q3UJS0\|Q | 0 | 2 | 2 |
| Activated spleen cDNA, RIKEN full-length enriched library, clone:F830112M22 product:ribosomal protein L3, full insert sequence - Mus musculus (Mouse) | Q3T9U9\|Q | 0 | 2 | 2 |
| Thioredoxin 1 - Mus musculus (Mouse) | A2AV97\|A | 0 | 2 | 2 |
| Ribosomal protein S20 - Mus musculus (Mouse) | Q5BLK2\|Q | 0 | 2 | 2 |
| Ribosomal protein S23 - Mus musculus (Mouse) | Q497E1\|Q | 0 | 2 | 2 |
| BAF53 :: cDNA, RIKEN full-length enriched library, clone:I920165I07 product:53 kDa BRG1-associated factor A - Mus musculus (Mouse) | Q3TF62\|Q | 0 | 2 | 2 |
| Bone marrow macrophage cDNA, RIKEN full-length enriched library, clone:I830018I23 product:ribosomal protein L7, full insert sequence - Mus musculus (Mouse) | Q3UBI6\|Q | 0 | 2 | 2 |
| 40S ribosomal protein S24 - Mus musculus (Mouse) | Q3TIF8\|Q: | 0 | 2 | 2 |
| Rplp1 protein - Mus musculus (Mouse) | Q58E35\|Q | 0 | 2 | 2 |
| Ribosomal protein L38 - Mus musculus (Mouse) | Q52KP0\|Q | 0 | 2 | 2 |
| cDNA, RIKEN full-length enriched library, clone:I920161F21 product:poly(rC) binding protein 2, full insert sequence - Mus musculus (Mouse) | Q3TF69\|Q | 0 | 2 | 2 |
| Ribosomal protein S26 - Mus musculus (Mouse) | Q497N1\|Q | 0 | 2 | 2 |
| CRL-1722 L5178Y-R cDNA, RIKEN full-length enriched library, clone:I730073G06 product:60S ribosomal protein L18a, full insert sequence - Mus musculus (Mouse) | Q3THJ0\|Q | 0 | 2 | 2 |
| Peroxiredoxin 1 - Mus musculus (Mouse) | B1AXW5\|E | 9 | 10 | 1 |
| Blastocyst blastocyst cDNA, RIKEN full-length enriched library, clone:I1C0038L22 product:eukaryotic translation elongation factor 2, full insert sequence - Mus musculus (Mouse) | Q3TK17\|Q | 5 | 6 | 1 |
| 10 day old male pancreas cDNA, RIKEN full-length enriched library, clone:1810006O06 product:RNA binding motif protein 3, full insert sequence - Mus musculus (Mouse) | Q545K5\|Q | 4 | 5 | 1 |
| Histone H4 - Mus musculus (Mouse) | Q61667\|Q | 3 | 4 | 1 |
| 60S ribosomal protein L6 - Mus musculus (Mouse) | Q3UCH0\|( | 3 | 4 | 1 |
| Ribosomal protein S8 - Mus musculus (Mouse) | Q497E9\|Q | 3 | 4 | 1 |
| 14-3-3 protein gamma subtype - Mus musculus (Mouse) | A8IP69\|A8 | 2 | 3 | 1 |
| Splicing factor, arginine/serine-rich 2 - Mus musculus (Mouse) | A2AA29\|A | 2 | 3 | 1 |
| Rps9 protein - Mus musculus (Mouse) | Q96EC0\|Q | 2 | 3 | 1 |
| Blastocyst blastocyst cDNA, RIKEN full-length enriched library, clone:I1C0007H08 product:ribosomal protein S2, full insert sequence - Mus musculus (Mouse) | Q3TL20\|Q | 2 | 3 | 1 |
| Bone marrow macrophage cDNA, RIKEN full-length enriched library, clone:I830164A20 product:actin, beta, cytoplasmic, full insert sequence - Mus musculus (Mouse) | Q3U5R4\|Q | 15 | 15 | 0 |
| Bone marrow macrophage cDNA, RIKEN full-length enriched library, clone:I830008E12 product:ribosomal protein S3, full insert sequence - Mus musculus (Mouse) | Q3UCL7\|Q | 7 | 7 | 0 |
| Poly A binding protein, cytoplasmic 4 - Mus musculus (Mouse) | A3KFU5\|A | 5 | 5 | 0 |
| 2 days neonate thymus thymic cells cDNA, RIKEN full-length enriched library, clone:E430010B17 product:ribosomal protein L4, cytosolic homolog - Mus musculus (Mouse) | Q564E8\|Q | 4 | 4 | 0 |
| TIB-55 BB88 cDNA, RIKEN full-length enriched library, clone:I730008D20 product:ribosomal protein L12, full insert sequence - Mus musculus (Mouse) | Q3TIQ2\|Q | 3 | 3 | 0 |
| Chromobox homolog 3 - Mus musculus (Mouse) | Q2YD72\|Q | 3 | 3 | 0 |
| Bone marrow macrophage cDNA, RIKEN full-length enriched library, clone:I830034K17 product:ribosomal protein S10, full insert sequence - Mus musculus (Mouse) | Q3U9P0\|Q | 2 | 2 | 0 |
| Ribosomal protein L18 - Mus musculus (Mouse) | Q0QEW9\| | 3 | 3 | 0 |
| Ribosomal protein L7a - Mus musculus (Mouse) | Q58ET1\|Q | 3 | 3 | 0 |

| | | | | |
|---|---|---|---|---|
| Rpl23a protein - Mus musculus (Mouse) | Q4V9X9\|Q | 3 | 3 | 0 |
| Rps28 protein - Mus musculus (Mouse) | Q059I1\|Q( | 2 | 2 | 0 |
| Ribosomal protein S6 - Mus musculus (Mouse) | Q5BLK1\|Q | 2 | 2 | 0 |
| 13 days embryo head cDNA, RIKEN full-length enriched library, clone:3110001F06 product:cofilin 1, non-muscle, full insert sequence - Mus musculus (Mouse) | Q544Y7\|Q | 2 | 2 | 0 |
| Ribosomal protein S15a - Mus musculus (Mouse) | Q5M9M4\|( | 2 | 2 | 0 |
| Rbmxrt protein - Mus musculus (Mouse) | Q91VM5\|Q | 2 | 2 | 0 |
| Ribosomal protein L23 - Mus musculus (Mouse) | A2A6F9\|A: | 2 | 2 | 0 |
| ES cells cDNA, RIKEN full-length enriched library, clone:2410026P17 product:ribosomal protein L14, cytosolic homolog - Mus musculus (Mouse) | Q9CWK0\|( | 2 | 2 | 0 |
| Adult male epididymis cDNA, RIKEN full-length enriched library, clone:9230011J09 product:ribosomal protein L24, full insert sequence - Mus musculus (Mouse) | Q3UW40\|( | 2 | 2 | 0 |
| Activated spleen cDNA, RIKEN full-length enriched library, clone:F830208A11 product:DEAD - Mus musculus (Mouse) | Q3T9L0\|Q | 2 | 2 | 0 |
| Ribosomal protein L31 - Mus musculus (Mouse) | Q5M9K9\|Q | 2 | 2 | 0 |
| Ribosomal protein L26 - Mus musculus (Mouse) | B1ARA3\|B | 2 | 2 | 0 |
| Tpm3 protein - Mus musculus (Mouse) | Q58E70\|Q | 13 | 12 | -1 |
| AHNAK - Mus musculus (Mouse) | Q6UL10\|Q | 7 | 6 | -1 |
| Npm1 protein - Mus musculus (Mouse) | Q5BL09\|Q | 8 | 7 | -1 |
| 60S ribosomal protein L13 - Mus musculus (Mouse) | Q5RKP3\|Q | 4 | 3 | -1 |
| Adult male liver tumor cDNA, RIKEN full-length enriched library, clone:C730027A09 product:Hypothetical RNA binding protein RDA288 homolog, full insert sequence - Mus musculus (Mouse) | Q3UEI6\|Q | 3 | 2 | -1 |
| Ribosomal protein S25 - Mus musculus (Mouse) | Q58EA6\|Q | 3 | 2 | -1 |
| 10 days neonate cerebellum cDNA, RIKEN full-length enriched library, clone:6530441M19 product:U6 SNRNA-ASSOCIATED SM-LIKE PROTEIN LSM6 homolog - Mus musculus (Mouse) | Q542U7\|Q | 3 | 2 | -1 |
| 15 days pregnant adult female placenta cDNA, RIKEN full-length enriched library, clone:I530024D06 product:annexin A7, full insert sequence - Mus musculus (Mouse) | Q3TJ49\|Q | 3 | 2 | -1 |
| Tcof1 protein - Mus musculus (Mouse) | Q05CS0\|Q | 7 | 5 | -2 |
| 13 days embryo liver cDNA, RIKEN full-length enriched library, clone:2510005B08 product:U6 snRNA-associated SM-like protein 4, full insert sequence - Mus musculus (Mouse) | Q9CY46\|Q | 4 | 2 | -2 |
| Tyrosine 3-monooxygenase/tryptophan 5-monooxygenase activation protein, theta polypeptide - Mus musculus (Mouse) | A3KML3\|A | 2 | 0 | -2 |
| Ribosomal protein L11 - Mus musculus (Mouse) | A2BH07\|A | 2 | 0 | -2 |
| Osteoclast-like cell cDNA, RIKEN full-length enriched library, clone:I420031E23 product:heat shock protein, A, full insert sequence - Mus musculus (Mouse) | Q3TW93\|( | 2 | 0 | -2 |
| CRL-1722 L5178Y-R cDNA, RIKEN full-length enriched library, clone:I730064N19 product:guanine nucleotide binding protein, beta 2, related sequence 1, full insert sequence - Mus musculus (Mouse) | Q3THP0\|Q | 2 | 0 | -2 |
| Retinoblastoma binding protein 4 - Mus musculus (Mouse) | A2A875\|A: | 2 | 0 | -2 |
| 17 days pregnant adult female amnion cDNA, RIKEN full-length enriched library, clone:I920090G16 product:Moloney leukemia virus 10, full insert sequence - Mus musculus (Mouse) | Q3TFC0\|Q | 2 | 0 | -2 |
| Rps19 protein - Mus musculus (Mouse) | Q5M9P3\|Q | 3 | 0 | -3 |
| MKIAA0670 protein - Mus musculus (Mouse) | Q80TU6\|Q | 3 | 0 | -3 |
| 40S ribosomal protein S12 - Mus musculus (Mouse) | Q6ZWZ6\|( | 4 | 0 | -4 |
| Muscle protein 684 - Mus musculus (Mouse) | Q9QYY3\|( | 4 | 0 | -4 |
| 2 days neonate thymus thymic cells cDNA, RIKEN full-length enriched library, clone:E430001E13 product:heat shock protein 8, full insert sequence - Mus musculus (Mouse) | Q3TEK2\|Q | 20 | 15 | -5 |

# Discussion

Early in ES differentiation, *Xist* spreads over the length of the X chromosome from which it is transcribed and transcriptionally silences the whole chromosome. The formation of this *Xist* covered chromosome territory is not sufficient for gene repression. Thus far, the mechanism and the factors that cooperate with *Xist* the initiation of gene silencing are presently unknown.

Here we established a protocol that allows to isolate defined nuclear fractions and to compare its protein content with and without *Xist* expression. We predicted to identify factors involved in the initiation of X chromosome inactivation in an unbiased manner by protein analysis of the *Xist* containing cell fraction. We established a biochemical fractionation procedure of the nuclear matrix fraction to detect proteins that become enriched upon X inactivation. Using this method followed by mass spectrometric analysis of protein samples we identified an enrichment of Trim28 in ES cells upon *Xist* expression among other candidates. Trim28 is especially interesting as it has been implicated in retroviral silencing in ES cells (Wolf and Goff, 2007). We confirmed our results by Western analysis suggesting an enrichment of Trim28 in the nuclear matrix, which is triggered by *Xist* expression in undifferentiated ES cells. It remains unclear if Trim28 is acting in gene silencing on the inactive X chromosome. This question could be addressed by expressing a silencing defective version of *Xist* that lacks the A-repeat. Genetic testing for a function of Trim28 in gene silencing by *Xist* is difficult as ES cells deficient in Trim28 have not yet been established.

Recruitment of Trim28 to the inactive X chromosome should further be investigated using immunofluorescence analysis. Colocalization of Trim28 with *Xist* could give further support to a role of Trim28 in X inactivation and would provide a potential link to antiviral host defence mechanisms.

Our method is suitable to be combined with advanced mass spectrometric measurements. Precise quantisation of protein amounts in nuclear fractions can be achieved using isotypic labelling of the samples with and without *Xist* induction. Approaches including SILAC will enable to characterize the changes in the chromosomal protein composition, which is triggered by *Xist*. This can potentially lead to the identification of factors that are crucial for *Xist* RNA localization, gene silencing and also maintenance of X inactivation. Albeit, an ever increasing number of factors are being identified, key components for explaining the mechanism of X inactivation are still missing. Direct biochemical approaches promise to fill in this missing information and advance our understanding of dosage compensation in mammals

# Material and Methods

## Cell culture of mouse ES cells

### Media

**MEFS (mouse embryonic feeder) medium**

450ml DMEM

50ml (10%) FCS

5ml L-Glutamnine (Sigma)

5ml non-essential amino acids (GIBCO)

5ml sodium pyruvate (sigma)

5ml penicillin streptomycin solution (GIBCO)

4µl ß-mercaptoethanol

filtered through Nalgene filter (pore size 0,2µm) and stored at 4°C

**ES-medium**

450ml DMEM

75ml (15%) FCS

5ml L-Glutamnine (Sigma)

5ml non-essential amino acids (GIBCO)

5ml sodium pyruvate (sigma)

5ml penicillin streptomycin solution (GIBCO)

4µl ß-mercaptoethanol

250µl LIF (500 Units/ml, leukemia inhibitory factor)

filtered through Nalgene filter (pore size 0,2µm) and stored at 4°C

**Retinoic acid differentiation (RADIF) - medium**

450ml DMEM

75ml (15%) FCS

5ml L-Glutamnine (Sigma)

5ml non-essential amino acids (GIBCO)

5ml sodium pyruvate (sigma)

5ml penicillin streptomycin solution (GIBCO)

4µl ß-mercaptoethanol

2µl retinoic acid

filtered through Nalgene filter (pore size 0,2µm) and stored at 4°C

ES cells were cultured in DMEM in the presence of 15% fetal calf serum (PAA, Austria), and 250 U of LIF/ml as described previously (Wutz and Jaenisch, 2000). Cultures were grown on mitotically inactivated mouse embryonic fibroblast feeder cells and passages every 3 days. Cells were rinsed twice with PBS (Ca Mg free) and then dissociated by treatment with 0.25% trypsin for 5 minutes at 37°C. Established ES cell lines were permanently stored in liquid nitrogen in cryotubes by adding 2xfreezing medium (20% DMSO; 80% fetal calf serum). For biochemical preparations ES cell cultures were cultured for 2 days on gelatine

(2%) coated plates without feeder cells. *Xist* was induced by the addition of 1µg/ml doxycycline (Sigma). Differentiating ES cells were cultured in DMEM containing 10% fetal calf serum (PAA, Austria) and differentiation was induced with 100nM all-*trans*-retinoic acid (Sigma).

## Immunofluorescence staining

For immunofluorescence ES cells were grown on Roboz slides (CellPoint Scientific, Gaithersburg, Maryland, United States) over night. The following steps were performed at RT. Briefly, cells were washed in PBS, fixed for 10 minutes in 4% PFA in PBS and permeabilzed for 5 minutes in 0,1% Na Citrate/ 0,1% Triton-X100 in water. Subsequently, cells were rinsed with PBS and blocked for 30 minutes in PBS containing 5% (wt/vol) BSA, 0,1% Tween-20. Thereafter cells were incubated for 2 hours with the primary antibody diluted in blocking solution, washed 3 times for 5 minutes with PBS containing 0,1% Tween and incubated for 1 hour with the secondary antibody, which was diluted 1:500 with blocking solution. Finally, cells were washed 2 times for 5 minutes with PBS containing 0,1% Tween, 5 minutes with PBS, incubated with PBS containing DAPI and mounted.

**The following antibodies were used:**

- Rabbit Sir2 (GeneTex, GTX12193)

  dilution: 1:50

- Rabbit Sirt1 (delta biolabs, C19)

  dilution: 1:50

- Goat Sirt1 (Santa Cruz Biotechnology, sc-19857)

  dilution: 1:50

- Rabbit Sirt1 (Santa Cruz Biotechnology, sc-15404)

  dilution: 1:50

- Rabbit Anti Sir2 (Sigma, S 5313)

  dilution: 1: 50

- Rabbit Sirt1 (abcam, ab12193)

  dilution: 1:50

- Rabbit Sirt1 (abccam, ab28170)

  dilution: 1:50

- Goat Sirt1 (abcam, ab53517)

  dilution: 1:50

- Rabbit Ash2 (bethyl, A300-107A)

## *Xist* fluorescence in situ hybridization

**Hybridizationbuffer**

1 part 20x SSC

2 parts 10mg/ml BSA

2 parts 50% dextran sulphate

Mixed and stored at -20°C

**Cytoskeletal buffer**

20ml 5M NaCl

102,7g sucrose

3ml 1M $MgCl_2$

10ml Pipes pH 6,8

to 1l with $H_2O$

### Generation of *Xist* RNA FISH probe

*Xist* RNA FISH probes were generated by random priming (Stratagene, La Jolla, Califorinia, United States) using Cy3-dCTP (Amersham). 100ng/µl of PGKΔ*Xist*PA was mixed with 22µl $H_2O$, and 10µl random primer, denatured for 5 minutes at 95°C and cooled on ice. Thereafter 10µl CTP-buffer, 0,5µl Cy3-dCTP and 1µl Klenow enzyme were added. The reaction mixture was incubated over night at 37°C. After stopping the reaction with 2µl EDTA (0,5M, pH 8), RNA fragments between 100 bp and 10 kb in length were purified using the QIAquick PCR Purification Kit. As final purification step, the probe was harvested in 30µl

TE-buffer and centrifuged for 5 minutes at 900rpm and 4°C. Subsequently, the probe was diluted in 20µl tRNA (20mg/ml), 20µl salmon sperm DNA (10mg/ml), 13µl (1/10V) 3M NaAc (pH 5,2) and 2,5V ethanol (absolute) and precipitated at -20°C over night. After centrifuging the probe at 13krpm, the pellet was washed twice with ethanol (absolute) and centrifuged for 5 minutes at 13krpm. The dry pellet was diluted in 80µl hybridization buffer, put for 10 mintues at 72°C, for 30 minutes at 37°C and stored at -20°C.

**Probe hybridization**

Cells were grown on robozslides, rinsed with PBS, extracted for 2 minutes with cytoskeletal buffer, rinsed with PBS and fixed for 10 minutes with 4% PFA. After cells were rinsed with 70% ethanol, several washing steps each for 5 minutes were performed: Cells were incubated in 70% ethanol, in 80% ethanol, in 95% ethanol and finally in 100% ethanol. Dry cells were hybridized over night at 37°C in a dark humid chamber with 4µl probe. Cells were washed in an agitating water bath at 37°C for 5 minutes 3 times with 2x SSC/ 50% formamide, for 5 minutes 3 times with 2x SSC, for 10 minutes with 1xSSC. Subsequently cells were washed for 5 minutes at room temperature with 4x SSC, stained for 5 minutes with 4x SSC + DAPI, washed for 5 minutes with 4x SSC and mounted.

## SDS-Polyacrylamide Gel Electrophoresis (SDS-PAGE) and Western blot analysis

### Buffers and Solutions

**4x TrisCl/SDS pH 6,8 (0,5M Tris.Cl, 0,4 % SDS)**

6,05g Tris base

40ml $H_2O$

pH 6,8 with 1M HCl

$H_2O$ to 100ml total V

2ml 20% SDS

filter through 0,45µm filter

**4x Tris.Cl/SDS pH 8,8 (1,5M Tris.Cl, 0,4% SDS)**

91g Tris base in 300ml $H_2O$

pH to 8,8 with 1M HCl

add 10ml 20% SDS

$H_2O$ to 500ml

filter through 0,45µm filter

**5x Tris- gly electrophoresis buffer**

25ml 20% SDS

15,1 Tris base

72g glycine

**Poneau solution**

0,2% Ponceau

5% acetic acid

**20x Transfer buffer**

58,6 glycine

116,2 g Tris base

37,5 ml 20% SDS

$H_2O$ to 1l

**1x Transfer buffer**

50ml 20x transfer buffer

200ml methanol

750ml $H_2O$

We prepared 9% of polyacrylamide gel for all protein analysis. The separating gel was poured, with isopropanol and polymerized. Then the isopropanol was removed and the stacking gel was added on the top of the separating gel. Protein samples were mixed with 6x loading buffer, boiled for 3 minutes at 95°C, spinned down and loaded into the wells. The protein amount according to nuclear matrix extraction analysis was always 1/10 of total sample. After running the gel at 25mA, the proteins were transferred over night at 4°C and 300mA using a stirrerto a nitrocellulose membrane. The blot was incubated in a poceau solution for some minutes and washed with PBS to test the protein transfer. Blocking was

performed for 30 minutes in an appropriate blocking solution (see usage of antibodies) and the first antibody was incubated for 2 hours in blocking solution. Washing steps and antibody incubations was performed in rolling falcon tubes. The membrane was washed 3 times for 5 minutes with PBS, 0,1% Tween and subsequently incubated for 1 hour with the secondary antibody (diltution: 1:10 000), horse raddish peroxidise coupled. The membrane was washed 3 times for 5 minutes with PBS, 0,1% Tween, rinsed with PBS, incubated for 1 minute with ECL detection solution and put in a plastic folder. Finally, the membrane was exposed for different times (starting with 5 seconds) to a luminescence sensitive film. The membranes were stored at -20°C.

**The following antibodies were used:**

- Rabbit Kap-1 (Trim28) Antibody (300 274A; Bethyl)

  blocking: 5% BSA, 0,1% Tween in PBS

  dilution: 1:10 000
- Rabbit polyclonal hnRNP U Antibody (ab20666, abcam)

  blocking: 3% milk powder, 0,1% Tween in PBS

  dilution: 0,4µg/µl
- Rabbit polyclonal to Histone H3 (ab1791, abcam)

  blocking: 5% BSA, 0,1% Tween in PBS

  dilution: 1:5000
- Rabbit Ash2 Antibody (A300-107A, Bethyl)

  blocking: 5% BSA, 0,1% Tween in PBS

  dilution: 1:10 000

## Nuclear Matrix extraction

### Buffers and Solutions

**Nuclei isolation (NI) Stock**

100mM Tris/HCl pH 7,4

10mM MgCl2

10mM CaCl2

2% NP40

1,6% Triton X100

**Nuclei isolation (NI) buffer** (prepared fresh before use)

1,6 ml NI-stock

0,4 ml Ficoll-Paque

2 µl 1M DMSO

1 mM 1M PMSF

**PRE – NI stock**

100 mM Tris/HCl pH7,4

10 mM $CaCl_2$

10 mM $MgCl_2$

**PRE – NI buffer**

1,6 ml PRE - NI-stock

0,4 Ficoll Paque

**DNase I buffer**

10mM PIPES pH6,8, 300mM sucrose, 50mM NaCl, 3mM MgCl2, 0,5% Triton X-100, 1mM CaCl2

**RNaseA buffer**

10mM Tris pH 7,0, 50mM NaCl, 3mM $MgCl_2$

**Nuclei isolation**

ES cells were cultivated with feeder cells, splitted and grown for 2 days to 90 – 95% confluency ($2x10^7$ cells) in a gelatine (2%) coated t75 flask without feeder cells. Cells were washed twice with PBS, trypsinized at 37°C 2-3 minutes with 1,5 ml trypsin and mixed with 15ml medium. Subsequently cells are centrifuged for 5 minutes at 900rcf, washed with PBS and diluted in 1ml medium. The following steps were performed at 4°C. Cells were overlaid onto 2ml cushion, centrifuged with increasing speed from 400rpm to 800rpm (30s/400rpm, 30s/500rpm, 30s/600rpm, 30s/700rpm, 6min/800rpm), and slowed down using the brake (Haraeus 2.0R Megafuge).

**Nuclear Matrix extraction of unfixed nuclei (continue with isolated nuclei)**

Nuclei were washed in DNase buffer, centrifuged for 5 minutes at 0,2 rcf. The nuclear pellet was resuspended in 100µl DNA buffer containing 10 Units DNAseI

(RNAse-free; Fermentas) and 1µl RNasin. DNA digestion was performed for 1 hour at 32°C. Subsequently, chromatin was extracted for 5 minutes on ice by the addition of 33,3 µl 1M ammonium sulphate to obtain a final concentration of 250mM ammonium sulphate. The samples were centrifuged for 5 minutes at 0,4g. The supernatant of the extraction with ammonium sulphate was stored for further analysis. The remaining pellet was resuspended in 200µl RNase buffer containing 9,6 µl RNase. RNA digestion was performed for 30 minutes at 4°C. The sample was centrifuged for 15 minutes at 4°C at 13krpm. The RNAse soluble supernatant and the insoluble pellet were stored at -20°C.

**Nuclear Matrix extraction of fixed nuclei (continue with isolated nuclei)**

Nuclei were resuspended in 700µl PRE-NI-buffer containing 1,4 µl 1M sodium tetrathionate (0,2mM total). After 1 minute, nuclei were centrifuged for 5 minutes at 0,2 g and washed with 1 ml DNase buffer. The sample was resuspended in 100 µl DNAse buffer containing 10 Units DNAse I (RNAse free, Fermentas) and 1µl RNAse inhibitor. DNA digestion was performed for 1 hour at 32°C. Subsequently, the chromatin was digested for 5 minutes at 4°C by the addition of 33,3 µl 1M ammonium sulphate (final c: 250mM ammonium sulphate). The sample was centrifuged for 5 minutes at 2g and washed with 1ml RNAse buffer (centrifugation: 5minutes, 2g). The pellet was digested for 30 minutes on ice with 9,6µg RNAse in 200µl RNAse buffer. Finally, 12µl 1M DTT (total c: 60mM) were added to the reaction mixture and incubated for another 15 minutes. The sample was centrifuged for 15 minutes at 4°C and the soluble fraction and the insoluble pellet was stored at -20°C.

# References


Akhtar, A. (2003). Dosage compensation: an intertwined world of RNA and chromatin remodelling. Curr Opin Genet Dev *13*, 161-169.

Augui, S., Filion, G.J., Huart, S., Nora, E., Guggiari, M., Maresca, M., Stewart, A.F., and Heard, E. (2007). Sensing X chromosome pairs before X inactivation via a novel X-pairing region of the Xic. Science *318*, 1632-1636.

Barr, M.L., and Bertram, E.G. (1949). A morphological distinction between neurones of the male and female, and the behaviour of the nucleolar satellite during accelerated nucleoprotein synthesis. Nature *163*, 676.

Berezney, R., and Coffey, D.S. (1974). Identification of a nuclear protein matrix. Biochem Biophys Res Commun *60*, 1410-1417.

Blewitt, M.E., Gendrel, A.V., Pang, Z., Sparrow, D.B., Whitelaw, N., Craig, J.M., Apedaile, A., Hilton, D.J., Dunwoodie, S.L., Brockdorff, N.*, et al.* (2008). SmcHD1, containing a structural-maintenance-of-chromosomes hinge domain, has a critical role in X inactivation. Nat Genet *40*, 663-669.

Borsani, G., Tonlorenzi, R., Simmler, M.C., Dandolo, L., Arnaud, D., Capra, V., Grompe, M., Pizzuti, A., Muzny, D., Lawrence, C.*, et al.* (1991). Characterization of a murine gene expressed from the inactive X chromosome. Nature *351*, 325-329.

Brockdorff, N., Ashworth, A., Kay, G.F., Cooper, P., Smith, S., McCabe, V.M., Norris, D.P., Penny, G.D., Patel, D., and Rastan, S. (1991). Conservation of position and exclusive expression of mouse Xist from the inactive X chromosome. Nature *351*, 329-331.

Brockdorff, N., Ashworth, A., Kay, G.F., McCabe, V.M., Norris, D.P., Cooper, P.J., Swift, S., and Rastan, S. (1992). The product of the mouse Xist gene is a 15 kb inactive X-specific transcript containing no conserved ORF and located in the nucleus. Cell *71*, 515-526.

Brown, C.J., Ballabio, A., Rupert, J.L., Lafreniere, R.G., Grompe, M., Tonlorenzi, R., and Willard, H.F. (1991a). A gene from the region of the human X inactivation centre is expressed exclusively from the inactive X chromosome. Nature *349*, 38-44.

Brown, C.J., Hendrich, B.D., Rupert, J.L., Lafreniere, R.G., Xing, Y., Lawrence, J., and Willard, H.F. (1992). The human XIST gene: analysis of a 17 kb inactive X-specific RNA that contains conserved repeats and is highly localized within the nucleus. Cell *71*, 527-542.

Brown, C.J., Lafreniere, R.G., Powers, V.E., Sebastio, G., Ballabio, A., Pettigrew, A.L., Ledbetter, D.H., Levy, E., Craig, I.W., and Willard, H.F. (1991b). Localization of the X inactivation centre on the human X chromosome in Xq13. Nature *349*, 82-84

.

Brown, C.J., Sekiguchi, T., Nishimoto, T., and Willard, H.F. (1989). Regional localization of CCG1 gene which complements hamster cell cycle mutation BN462 to Xq11-Xq13. Somat Cell Mol Genet *15*, 93-96.

Brown, S.D. (1991). XIST and the mapping of the X chromosome inactivation centre. Bioessays *13*, 607-612.

Chaumeil, J., Le Baccon, P., Wutz, A., and Heard, E. (2006). A novel role for Xist RNA in the formation of a repressive nuclear compartment into which genes are recruited when silenced. Genes Dev *20*, 2223-2237.

Chaumeil, J., Okamoto, I., Guggiari, M., and Heard, E. (2002). Integrated kinetics of X chromosome inactivation in differentiating embryonic stem cells. Cytogenet Genome Res *99*, 75-84.

Clemson, C.M., McNeil, J.A., Willard, H.F., and Lawrence, J.B. (1996). XIST RNA paints the inactive X chromosome at interphase: evidence for a novel RNA involved in nuclear/chromosome structure. J Cell Biol *132*, 259-275.

Csankovszki, G., Nagy, A., and Jaenisch, R. (2001). Synergism of Xist RNA, DNA methylation, and histone hypoacetylation in maintaining X chromosome inactivation. J Cell Biol *153*, 773-784.

Csankovszki, G., Panning, B., Bates, B., Pehrson, J.R., and Jaenisch, R. (1999). Conditional deletion of Xist disrupts histone macroH2A localization but not maintenance of X inactivation. Nat Genet *22*, 323-324.

de Napoles, M., Mermoud, J.E., Wakao, R., Tang, Y.A., Endoh, M., Appanah, R., Nesterova, T.B., Silva, J., Otte, A.P., Vidal, M.*, et al.* (2004). Polycomb group proteins Ring1A/B link ubiquitylation of histone H2A to heritable gene silencing and X inactivation. Dev Cell *7*, 663-676.

Ekwall, K. (2005). Genome-wide analysis of HDAC function. Trends Genet *21*, 608-615.

Fackelmayer, F.O. (2005). A stable proteinaceous structure in the territory of inactive X chromosomes. J Biol Chem *280*, 1720-1723.

Gossen, M., Freundlieb, S., Bender, G., Muller, G., Hillen, W., and Bujard, H. (1995). Transcriptional activation by tetracyclines in mammalian cells. Science *268*, 1766-1769.

Guarente, L. (1999). Diverse and dynamic functions of the Sir silencing complex. Nat Genet *23*, 281-285.

Heard, E., Rougeulle, C., Arnaud, D., Avner, P., Allis, C.D., and Spector, D.L. (2001). Methylation of histone H3 at Lys-9 is an early mark on the X chromosome during X inactivation. Cell *107*, 727-738.

Helbig, R., and Fackelmayer, F.O. (2003). Scaffold attachment factor A (SAF-A) is concentrated in inactive X chromosome territories through its RGG domain. Chromosoma *112*, 173-182.

Herzing, L.B., Romer, J.T., Horn, J.M., and Ashworth, A. (1997). Xist has properties of the X-chromosome inactivation centre. Nature *386*, 272-275.

Keohane, A.M., O'Neill L, P., Belyaev, N.D., Lavender, J.S., and Turner, B.M. (1996). X-Inactivation and histone H4 acetylation in embryonic stem cells. Dev Biol *180*, 618-630.

Kohlmaier, A., Savarese, F., Lachner, M., Martens, J., Jenuwein, T., and Wutz, A. (2004). A chromosomal memory triggered by Xist regulates histone methylation in X inactivation. PLoS Biol *2*, E171.

Kustatscher, G., Hothorn, M., Pugieux, C., Scheffzek, K., and Ladurner, A.G. (2005). Splicing regulates NAD metabolite binding to histone macroH2A. Nat Struct Mol Biol *12*, 624-625.

Leeb, M., and Wutz, A. (2007). Ring1B is crucial for the regulation of developmental control genes and PRC1 proteins but not X inactivation in embryonic cells. J Cell Biol *178*, 219-229.

Liou, G.G., Tanny, J.C., Kruger, R.G., Walz, T., and Moazed, D. (2005). Assembly of the SIR complex and its regulation by O-acetyl-ADP-ribose, a product of NAD-dependent histone deacetylation. Cell *121*, 515-527.

Lyon, M.F. (1961). Gene action in the X-chromosome of the mouse (Mus musculus L.). Nature *190*, 372-373.

Marahrens, Y., Loring, J., and Jaenisch, R. (1998). Role of the Xist gene in X chromosome choosing. Cell *92*, 657-664.

Marahrens, Y., Panning, B., Dausman, J., Strauss, W., and Jaenisch, R. (1997). Xist-deficient mice are defective in dosage compensation but not spermatogenesis. Genes Dev *11*, 156-166.

Meyer, B.J. (2000). Sex in the wormcounting and compensating X-chromosome dose. Trends Genet *16*, 247-253.

Morey, C., Navarro, P., Debrand, E., Avner, P., Rougeulle, C., and Clerc, P. (2004). The region 3' to Xist mediates X chromosome counting and H3 Lys-4 dimethylation within the Xist gene. EMBO J *23*, 594-604.

Morishima, A., Grumbach, M.M., and Taylor, J.H. (1962). Asynchronous duplication of human chromosomes and the origin of sex chromatin. Proc Natl Acad Sci U S A *48*, 756-763.

Nesterova, T.B., Slobodyanyuk, S.Y., Elisaphenko, E.A., Shevchenko, A.I., Johnston, C., Pavlova, M.E., Rogozin, I.B., Kolesnikov, N.N., Brockdorff, N., and Zakian, S.M. (2001). Characterization of the genomic Xist locus in rodents reveals conservation of overall gene structure and tandem repeats but rapid evolution of unique sequence. Genome Res *11*, 833-849.

Ohhata, T., Tachibana, M., Tada, M., Tada, T., Sasaki, H., Shinkai, Y., and Sado, T. (2004). X-inactivation is stably maintained in mouse embryos deficient for histone methyl transferase G9a. Genesis *40*, 151-156.

Ohno, S., and Hauschka, T.S. (1960). Allocycly of the X-chromosome in tumors and normal tissues. Cancer Res *20*, 541-545.

Okamoto, I., Otte, A.P., Allis, C.D., Reinberg, D., and Heard, E. (2004). Epigenetic dynamics of imprinted X inactivation during early mouse development. Science *303*, 644-649.

Penny, G.D., Kay, G.F., Sheardown, S.A., Rastan, S., and Brockdorff, N. (1996). Requirement for Xist in X chromosome inactivation. Nature *379*, 131-137.

Plath, K., Fang, J., Mlynarczyk-Evans, S.K., Cao, R., Worringer, K.A., Wang, H., de la Cruz, C.C., Otte, A.P., Panning, B., and Zhang, Y. (2003). Role of histone H3 lysine 27 methylation in X inactivation. Science *300*, 131-135.

Rastan, S. (1983). Non-random X-chromosome inactivation in mouse X-autosome translocation embryos--location of the inactivation centre. J Embryol Exp Morphol *78*, 1-22.

Rastan, S., and Robertson, E.J. (1985). X-chromosome deletions in embryo-derived (EK) cell lines associated with lack of X-chromosome inactivation. J Embryol Exp Morphol *90*, 379-388.

Robyr, D., Suka, Y., Xenarios, I., Kurdistani, S.K., Wang, A., Suka, N., and Grunstein, M. (2002). Microarray deacetylation maps determine genome-wide functions for yeast histone deacetylases. Cell *109*, 437-446.

Rougeulle, C., and Avner, P. (2003). Controlling X-inactivation in mammals: what does the centre hold? Semin Cell Dev Biol *14*, 331-340.

Russell, L.B. (1963). Mammalian X-chromosome action: inactivation limited in spread and region of origin. Science *140*, 976-978.

Sado, T., Fenner, M.H., Tan, S.S., Tam, P., Shioda, T., and Li, E. (2000). X inactivation in the mouse embryo deficient for Dnmt1: distinct effect of hypomethylation on imprinted and random X inactivation. Dev Biol *225*, 294-303.

Savarese, F., Flahndorfer, K., Jaenisch, R., Busslinger, M., and Wutz, A. (2006). Hematopoietic precursor cells transiently reestablish permissiveness for X inactivation. Mol Cell Biol *26*, 7167-7177.

Schoeftner, S., Sengupta, A.K., Kubicek, S., Mechtler, K., Spahn, L., Koseki, H., Jenuwein, T., and Wutz, A. (2006). Recruitment of PRC1 function at the initiation of X inactivation independent of PRC2 and silencing. EMBO J *25*, 3110-3122.

Silva, J., Mak, W., Zvetkova, I., Appanah, R., Nesterova, T.B., Webster, Z., Peters, A.H., Jenuwein, T., Otte, A.P., and Brockdorff, N. (2003). Establishment of histone h3 methylation on the inactive X chromosome requires transient recruitment of Eed-Enx1 polycomb group complexes. Dev Cell *4*, 481-495.

Simon, J.A., and Tamkun, J.W. (2002). Programming off and on states in chromatin: mechanisms of Polycomb and trithorax group complexes. Curr Opin Genet Dev *12*, 210-218.

Takagi, N., Sugawara, O., and Sasaki, M. (1982). Regional and temporal changes in the pattern of X-chromosome replication during the early post-implantation development of the female mouse. Chromosoma *85*, 275-286.

Wolf, D., and Goff, S.P. (2007). TRIM28 mediates primer binding site-targeted silencing of murine leukemia virus in embryonic cells. Cell *131*, 46-57.
Wutz, A. (2003). RNAs templating chromatin structure for dosage compensation in animals. Bioessays *25*, 434-442.

Wutz, A., and Jaenisch, R. (2000). A shift from reversible to irreversible X inactivation is triggered during ES cell differentiation. Mol Cell *5*, 695-705.

Wutz, A., Rasmussen, T.P., and Jaenisch, R. (2002). Chromosomal silencing and localization are mediated by different domains of Xist RNA. Nat Genet *30*, 167-174.

# CURRICULUM VITAE – RENATE HÄRTEL

## PERSONAL DETAILS

| | |
|---|---|
| Name: | Renate Ingrid Härtel |
| Home address: | Urbangasse 12/9, 1170 Vienna, Austria |
| Telephone: | 0699/11 810 745 |
| Email: | renate@haertel.at |
| Date of birth: | March 6th 1981 |
| City of birth: | Vienna |
| Nationality: | Austria |
| Family status: | Single |

## EDUCATION AND QUALIFICATIONS

| | |
|---|---|
| 2000 – present | **University of Vienna, Austria**<br>Degree: Molecular Biology (A490)<br>Main subjects: cell biology, genetics, neurobiology |
| 1991 – 1999 | **Bundesrealgymnasium Maroltingergasse (Grammer School), Vienna**<br>Scientific direction, focus on biology, physics and chemistry<br>Matura (A-levels, general qualification for university entrance) |

## PROFESSIONAL EXPERIENCE

| | |
|---|---|
| June, August 2002 | **Children's Cancer Research Institute,**<br>Minimal residual disease studies in childhood leukaemia |
| June 2000 - December 2003 | **Erste Bank,**<br>Department: product management and financing |
| June 2001 | **Baxter AG,**<br>Quality control |
| Spring 2000 | **Restaurant DO & CO,**<br>Reception |
| August, September 1999 | **Gerot Pharma GmbH,**<br>Manufacturing |

## PRACTICAL COURSES

- **University of Vienna, Department of Molecular Cell Biology,**

  Univ. Prof. Friedrich Propst
  Theme:
  Colocalization of MAP(microtubule associated protein) 1B on cellular level (cell lines: N2a, Ptk2, 3T3)

- **Brain Research Institute, Department of Neuronal Cell Biology,**

  Head: Univ. Prof. Michael Kiebler, Supervisor: Dr. Paolo Macchi
  Themes:
  - Subcellular localization of Pum (Pumilio)2 mRNA in primary culture of hippocampal neurons
  - Cloning and over expression of Pum2 tagged with EYFP in primary culture

- **Basics of Neuroscience, Brain Research Institute,**

  Laboratory course teaching techniques used in neurobiology

## TECHNICAL SKILLS

- Western blot
- Cell culture
- Plasmid isolation
- cDNA cloning
- *In vitro* RNA transcription
- Purification of RNA
- Fluorescence *in situ* hybridization
- RT-PCR, screening PCR
- Lipid transfection, $Ca^{2+}$-phosphate transfection
- Immunostaining

## OTHER RELEVANT SKILLS

| | |
|---|---|
| IT Skills | • Windows 2000 (Word, Excel, Powerpoint)<br>• Photoshop |
| Languages | • German (fluent)<br>• English (fluent), Pitman Examination, standard: higher intermediate<br>• French<br>• Spanish |
| Other | • Driving licence |

## INTERESTS

- Sports (skiing, jogging, swimming)
- Music
- Travelling (different cultures)